이학석사 학위논문

Numerical Integration for Neutron Star Binaries in Eccentric Orbits

타원 궤도를 돌고 있는 중성자 별 쌍성의 수치 상대론적 계산

2018년 2월

서울대학교 대학원

물리·천문학부 천문학전공

박 관 호

Numerical Integration for Neutron Star Binaries in Eccentric Orbits

타원 궤도를 돌고 있는 중성자 별 쌍성의 수치 상대론적 계산

지도교수 이 형 목

이 논문을 이학석사 학위논문으로 제출함

2018년 4월

서울대학교 대학원

물리·천문학부 천문학전공

박 관 호

박 관 호의 이학석사 학위논문을 인준함

2017년 12월

위 원 장 _____

부 위 원 장 _____

위 원 _____

Numerical Integration for Neutron Star Binaries in Eccentric Orbits

by

Kwan Ho Park
(nobel@astro.snu.ac.kr)

A dissertation submitted in partial fulfillment of the requirements for the degree of

Master of Science

in

Astronomy

in

Astronomy Program
Department of Physics and Astronomy
Seoul National University

Committee:

Professor Woong Tae Kim

Professor Hyung Mok Lee

Professor Hyun Kyu Lee

ABSTRACT

This dissertation try to focus on new paradigm of initial data and its evolution for Einstein's field equation when spacetime has matter field. To make proper initial data, we carry out test employing boosted Tolmann-Oppenhiemmer-Volkoff(TOV) star. TOV star assumes perfect fluid obeying polytropic process and metric keeps spherical symmetry. It is static and stationary solution so it shows stable maximum density oscillation. On the other hand, when TOV star got boosted, maximum density oscillation become excited. Such a behaviour provide good hint for error which will arise at binary system.

We presents initial data for binary in the eccentric orbit employing double TOV stars. Rotation configuration in the binary should have vanishing vorticity. To deal with such a configuration, constant coordinate velocity approximation is utilized. Moreover, initial external field due to companion is ignored because we want to look at contribution of relativistic hydrodynamics part. So, metric combination is not superposition but sewing TOV solution at the boundary line containing origin. We simply compare initial data of us and `LORENE` initial data which solves constraints equations via multi grid method. Key difference is high frequency mode of density oscillation and gravitational wave due to surface mode of neutron star.

While binary system is evolving, spurious oscillation occurs around 500 coordinate time when eccentricity is about 0.17. According to result of boosted TOV star, boost parameter might be attributed to such as oscillation and pressure perturbation is applied to treat the problems. Because boost can spoil relativistic equilibrium, we use strong Bernuolli's theorem which assert homogeneous injection energy to renew equilibrium. For highly eccentric orbit, stars collide each other before showing spurious oscillation. Though perturbed binary delivers relived maximum density oscillation, other part is excited at last $6,7$ percent. Relatively high constraint violation is remained problem but it can be resolved by smoothing lapse function and metric at boundary line.

Keywords: neutron star: initial and evolution − neutron star: binary system − neu-

tron star: equilibrium − neutron star: numerical relativity

Student Number: 2014-22382

Contents

Chapter 1

Introduction

Einstein's field equation of general relativity imposes distinctive interpretation on gravity in geometrical language. The Einstein's gravity expect somewhat different character like gravitational wave or orbit precessing, which can not be described by Newtonian gravity. Particularly, gravitational wave can deliver information of compact object or cosmological scaled thing that cannot resolve using electromagnetic wave. It means that gravitational wave is able to open another window searching the Universe. In fact, it is predicted by Einstein about 100 years ago but the first success of observation is recently achieved. Laser Interferometer Gravitational wave Observatory(LIGO hereafter) see first gravitational wave from black hole binary(Abott et al. 2016) via matched filtering method in 2015. Then, more events are observed successively for black hole binary and in 2017, gravitational wave from neutron star binary is captured(Abott et al. 2017). Due to its small mass and complex behaviour after merge comparing with black hole, only inspiral phase is obtained. Matched filtering method(Owen and Sathyaprakash 1999), key method for observing gravitational wave, strongly depends on gravitational wave form. This wave form is calculated by numerical relativity solving Einstein's field equation. Therefore accurate wave form need accurate numerical relativity simulation. Though there is alternative way to estimate gravitational wave much faster than numerical relativity like post Newtonian, that is black hole binary story. Starting from late inspiral, neutron star binary shows very complex and violent phenomenon and such

a dynamics cannot be resolved without relativistic computation code. So numerical relativity is not substitution acceptable in current knowledge. The general relativity is constrained system which physically requires initial data before evolving. It is natural that fairly exact initial data lead to correct evolution so precise initial data construction should be primary goal. LORENE(Gourgoulhon et al. 2001) and SGRID(Tichy 2009) already prepared differential equation solver for initial data. Unfortunately, they can cover quasi circular orbit, not eccentric one. In Newtonian limit, it is easy problem that make circular orbit eccentric by reducing angular momentum. However, it is not trivial problem in general relativistic case. Because of difficulty to construct initial data for eccentric orbit, Gold et al. (2012) firstly propose numerical trick to describe the orbit. By locating TOV star far away(about 200km), they can ignore severe problem that can occur. When the separation is small, unphysical behaviour like spurious oscillation or relatively large constraint violation arise. Tsatsin and Marronetti (2013) showed relieved oscillation through over-contraction and rescaling but their method seems to be add-hoc. Moldenhauer et al. (2014) carried out more developed study for initial data of eccentric orbit via solving constraint equation. They state that problem is how to define stationarity of eccentric orbit and remodel helical vector as heliptical vector. Objective of this paper is building initial data for eccentric orbit in simple way. Main focus in not spacetime variable but contribution of hydro variable. Though constraint equations are not solved in the paper, another treatments will be asserted. Pressure perturbation with respect to strong relativistic Bernoulli's theorem will be applied to relieve spurious oscillation. Additional factors of static and stationary TOV star spoil original equilibrium. It is expected that renewed pressure profile is able to stand for new equilibrium

configuration. The convention and notation used in this paper are following.

- The metric convention is $(-,+,+,+)$
- The units set $c = G = M_{sun} = 1$ which represents 1.47km in length, 4.92×10^{-3} ms in time and 1.99×10^{30} kg in mass.
- The Greek indcies $(\mu, \nu, \lambda, \cdots)$ mean four dimensional component from 0 to 3.
- The Latin indcies $(i, j, k, \cdots)$ mean three dimensional component from 1 to 3.

The overall contents of dissertation consist of 6 chapters. Chapter 2 will introduce basic concept of relativistic theories for spacetime and hydrodynamics. It will also provide mathematical preliminaries that frequently utilized in numerical relativity and relativistic fluid configuration to deal with stellar structure. Computational method and its code implementation will be introduced in chapter 3. It briefly explains network of Cactus code. Numerical relativity simulation for single star is shown in chapter 4. There are two examples, one is static and stationary state solution and the other is boosted star. Chapter 5 treats initial data for binary system in earnest. It will explain hypothesis employed and show how it is valid. Finally, chapter 6 summarize that strategy of this paper with conclusion. It also notes remained problem which do not dealing with yet.

Chapter 2

Relativistic theories

This chapter will explain basic formalism based on general relativity. Compact stars are composed of dense matter and this matter makes curvature. So, dynamic equation describing motion of matter, for instance hydrodynamics or thermodynamics, should be modified by general relativistic perspective. First, ADM 3+1 formalism show that how to split four dimensional quantities and second, relativistic hydrodynamics cover equation of motion for fluid particle, which is different from test particle.

2.1 ADM 3+1 formalism

General relativity treats scalar, vector and tensor field in four dimensional manifold called spacetime. Due to its complexity, method of decomposition into smaller dimension is employed. Typically, numerical calculation for general relativity engaging in compact star or its binaries usually utilize 3+1 decomposition where 3 for three dimensional hypersurface and 1 for one dimensional coordinate time. This section is going to explain basic idea of ADM 3+1 formalism in simple way.

2.1.1 Mathematical preliminaries

Before conducting the idea for 3+1 splitting, it is necessary that containing mathematical building blocks. Starting from forms and vectors, differential operators such that

lie derivative, exterior derivative and covariant derivative which are more useful than partial derivative will be introduced.

N form and N vector are nothing but tensor whose rank type is $(0, N)$ and $(N, 0)$ respectively. Mathematically speaking, tensor is abstract quantity in tensor space which is multi product of vector spaces. However, priority is intuition how to treat such abstract things. Thinking about matrix, two dimensional box filled with numbers. That is one example for tensor of rank 2. Then rank 3, 4 or N tensor may be N dimensional box which contains N^N components. Form and vector can reduce their rank through contraction with vector and form. Volume q form, kind of unit form, can provide mapping such that converting p form to $q - p$ vector. This mapping is called dual. All of physical quantity in general relativity is described by tensor formulation and next step is find way to measure difference of those things. Differential operator is able to help such a comparison.

Mathematical structure of general relativity is different from Newtonian mechanics and special relativity. Arbitrary point a on the manifold can build up four dimensional vector space called tangent space. Vectors in different vector space intrinsically cannot interact (measure difference of vectors , for example) each other so something relevant instrument is needed. To deal with this, Lie derivative, Exterior derivative and Covariant derivative is necessary. Lie and exterior derivative are composed of intrinsic nature of manifold but covariant derivative create external structure called connection (Gourgoulhon 2006).

First of all, lie derivative is frequently used in fluid dynamics to find difference of quantity along the flow line. Employing flow vector field $\mathbf{u}$ and setting arbitrary vector field $\mathbf{v}$ to figure out the difference between $\mathbf{v}(a)$ and $\mathbf{v}(b)$, where point b is neighbouring point a as in figure. Let's define mapping of point a along flow $\mathbf{u}$ infinitesimally, $\psi_\epsilon(a)$, that is equivalent to point b. Then pick up some point on the vector field $\mathbf{v}(a)$, let that point a' in the figure. The vector $\mathbf{aa'}$ is part of $\mathbf{v}(a)$ so, it is $c\mathbf{v}(a)$. Like $b = \psi_\epsilon(a)$, mapping of $c\mathbf{v}(a)$, $\psi_\epsilon(c\mathbf{v})$, connect to point b' which is image $\psi_\epsilon(a')$. Now it is possible to compare vector field $\mathbf{v}$ at point q and at point p dragged along flow field $\mathbf{u}$. By vector

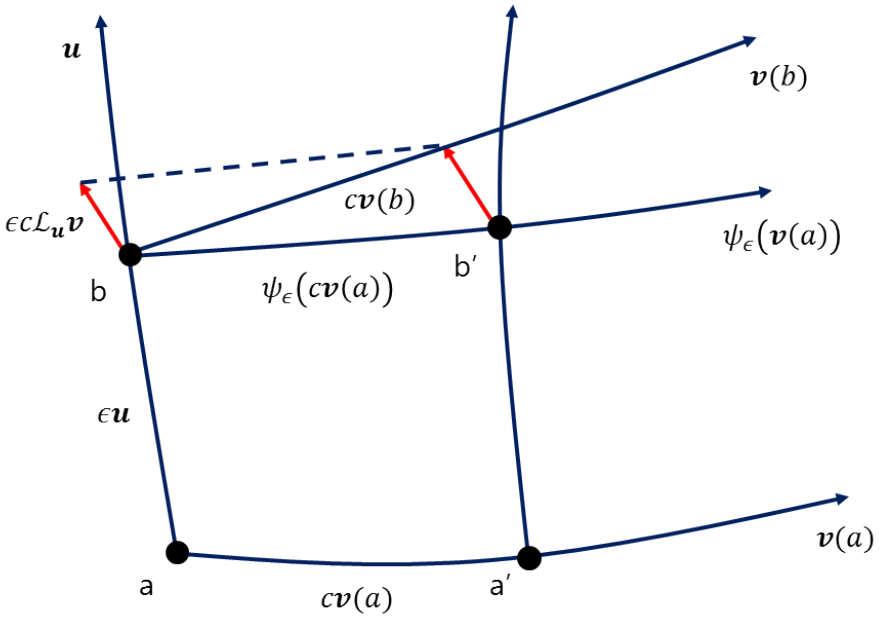

Figure 2.1: Lie derivative description. ψ_ϵ is mapping between point a and b.

identity,

$$c\epsilon\mathcal{L}_{\mathbf{u}}\mathbf{v} = c\mathbf{v}\left(b\right) - c\psi_\epsilon\left(\mathbf{v}\left(a\right)\right) \tag{2.1}$$

Therefore, lie derivative is defined as

$$\mathcal{L}_{\mathbf{u}}\mathbf{v} = \lim_{\epsilon\to 0}\frac{\mathbf{v}\left(b\right) - \psi_\epsilon\left(\mathbf{v}\left(a\right)\right)}{\epsilon} \tag{2.2}$$

For N form and N vector when $N = 1$,

$$\mathcal{L}_{\mathbf{u}}v^\alpha = u^\mu\frac{\partial v^\alpha}{\partial x^\mu} - v^\mu\frac{\partial u^\alpha}{\partial x^\mu} \tag{2.3}$$

$$\mathcal{L}_{\mathbf{u}}\omega_\alpha = u^\mu\frac{\partial \omega_\alpha}{\partial x^\mu} + \omega_\mu\frac{\partial u^\mu}{\partial x^\alpha} \tag{2.4}$$

Note that lie derivative gives combination of partial derivative. It sometimes lead to simpler way while estimating covariant derivative, which will be understood later. One more thing, several text books say push forward and pull backward as mathematical terminology. Though those are not mentioned, process description above is exactly same thing to push forward or pull backward.

Next is exterior derivative, differential operator for N form. Due to their mathematical origin, they are antisymmetric in all of the operation. The exterior derivative of N form $\boldsymbol{\pi}$ gives $(N+1)$ form $\mathbf{d}\boldsymbol{\pi}$. For example,

$$1 \text{ form } \pi_\alpha \quad : \quad (\mathbf{d}\boldsymbol{\pi})_{\alpha\beta} = \frac{\partial \pi_\beta}{\partial x^\alpha} - \frac{\partial \pi_\alpha}{\partial x^\beta} \tag{2.5}$$

$$2 \text{ form } \pi_{\alpha\beta} \quad : \quad (\mathbf{d}\boldsymbol{\pi})_{\alpha\beta\gamma} = \frac{\partial \pi_{\beta\gamma}}{\partial x^\alpha} + \frac{\partial \pi_{\gamma\alpha}}{\partial x^\beta} + \frac{\partial \pi_{\alpha\beta}}{\partial x^\gamma} \tag{2.6}$$

Intuitively speaking, this derivative provides boundary points of the N form or type $(0, N)$ tensor.(see Misner et al. 1973 for more explanation) With this idea, boundary point of boundary point become zero. This fact means that exterior derivative of exterior derivative is vanished.

$$\mathbf{d}\mathbf{d}\boldsymbol{\pi} = 0 \tag{2.7}$$

Also, it can apply to Stokes's theorem,

$$\oint_{\partial \mathcal{D}} \boldsymbol{\pi} = \int_{\mathcal{D}} \mathbf{d}\boldsymbol{\pi} \tag{2.8}$$

From figure below, the number of captured field points by boundary of domain is equivalent to the number of points in the domain. Another useful identity is Cartan

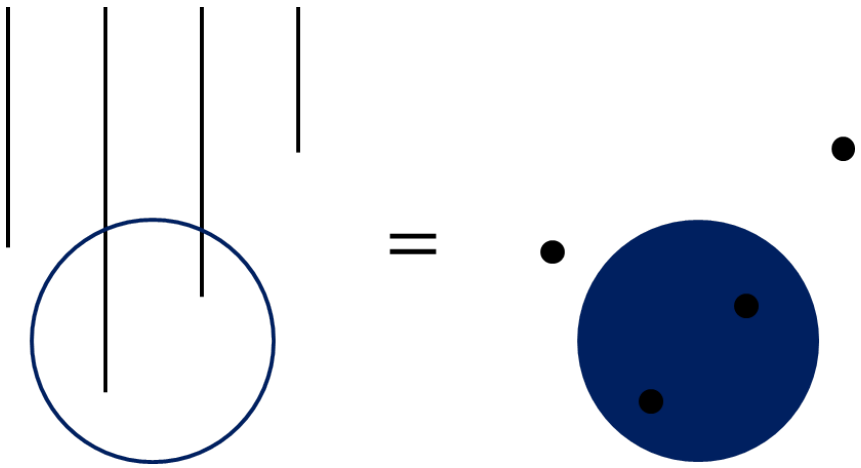

Figure 2.2: Schematic description for Stokes's theorem. Lines are arbitrary form, $\boldsymbol{\pi}$, and points are its exterior derivative, $\mathbf{d}\boldsymbol{\pi}$.

identity, it postulates lie derivative of N form $\boldsymbol{\pi}$ along vector $\mathbf{u}$ is

$$\mathcal{L}_{\mathbf{u}}\boldsymbol{\pi} = \mathbf{u} \cdot \mathbf{d}\boldsymbol{\pi} + \mathbf{d}\left(\mathbf{u} \cdot \boldsymbol{\pi}\right) \tag{2.9}$$

Of course, it can be related to covariant derivative. It will be employed in relativistic hydrodynamics part to deal with constrained conditions.

The last, covariant derivative finds variation of tensor field when mathematical structure called affine connection exist. Lie derivative defines intrinsic linear map and flow vectors between point a and neighbourhood b but connection contribute to similar thing in covariant derivative. Let the variation of vector field $\mathbf{v}$ at near two points a and b. It is defined by

$$\delta\mathbf{v} = \boldsymbol{\nabla}_{\overrightarrow{\mathbf{ab}}}\mathbf{v} \tag{2.10}$$

When vector moves parallelly to itself along the vector $\overrightarrow{\mathbf{ab}}$ and vanishing $\delta\mathbf{v}$, it is said parallel transport. Note that there is no preferred connection in general relativity but one can be chosen for convenience. The observers in inertial frame whose four acceleration is 0,

$$u^{\mu}\nabla_{\mu}u^{\nu} = 0 \tag{2.11}$$

its four velocity is tangent vector of geodesics with respect to metric field $g_{\mu\nu}$ and it is parallelly transported along itself to geodesics. This fact can provide unique one, called Levi-Civita connection. This connection has special property as following.

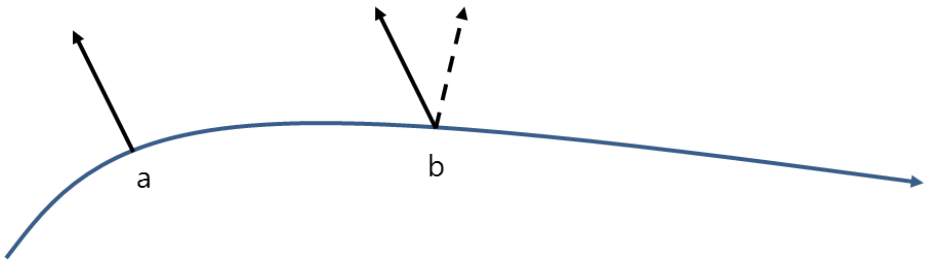

Figure 2.3: If arbitrary vector at point a is transported parallelly, it is showed as bold arrow at point b. If not, direction of the vector is changed as dashed arrow.

$$\nabla_{\alpha}g_{\beta\gamma} = 0 \tag{2.12}$$

For example, covariant derivative of 1-form in coordinate bases is

$$\nabla_\alpha \pi_\beta = \frac{\partial \pi_\beta}{\partial x^\alpha} - \Gamma^\lambda_{\alpha\beta}\pi_\lambda \tag{2.13}$$

2.1.2 Spacetime foliation

It's time to look at mathematical structure of general relativity more precisely. Imagine three dimensional object, for example a loaf of bread, and slice it with infinitesimally small thickness. Each slice is a part of original bread and its shape is depend on slicing method. In ADM 3+1 formalism, it slices four dimensional manifold like a loaf of bread. Sliced one is called time slice, hypersurface or foliation. By intuition, spacetime can be expressed by union of foliation.

$$\mathcal{M} = \bigcup_{t\in\mathbb{R}} \Sigma_t \tag{2.14}$$

Difference between bread and manifold is dimension, one more dimension for time. A unit vector normal to hypersurface is defined as

$$n_\mu = -\alpha \nabla_\mu t \tag{2.15}$$

Here, α represents lapse function. From unit normal vector, normal evolution vector is

$$\mathbf{m} = \alpha \mathbf{n} \tag{2.16}$$

A coordinate observer whose four velocity is unit normal vector $n^\mu = -\alpha dt$ is eulerian observer or normal observer. Note that dt is time vector so don't be confused with exterior derivative. Acting time derivative on four velocity of eulerian observer, its four acceleration is following.

$$\begin{aligned} a_\mu &= n^\nu \nabla_\nu n_\mu & (2.17)\\ &= \frac{1}{\alpha}\gamma^\nu_\mu \nabla_\nu \alpha & (2.18) \end{aligned}$$

where $\gamma^\nu_\mu = \delta^\nu_\mu + n^\nu n_\mu$ working as spatial projection operator. Except homogeneous lapse function, normal observer has non-vanishing four acceleration. So it is not on geodesics. On the other hand, each time slice need to set up coordinate system to solve PDE such

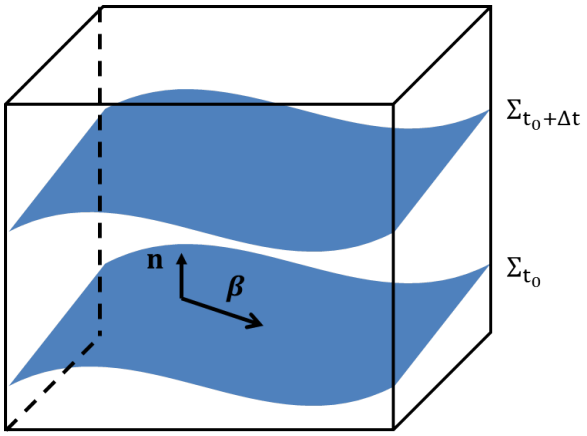

Figure 2.4: Hypersurface foliated in spacetime. Normal evolution is lie derivative along the normal evolution vector **m** and coordinate time evolution is lie dragging along ∂_t.

as constraint equations(this will be introduced later) or other things. If they provides smooth coordinate to next level surface, that is well behaved coordinate system. Such a good coordinate is keeping same spatial coordinate on the hypersurface. Now defining ∂_t which is tangent vector of $x^i = const.$ world line. The difference between normal evolution vector m^μ and coordinate time vector ∂_t is shift vector β^μ. Therefore,

$$\partial_t = m^\mu + \beta^\mu \tag{2.19}$$

Rearranged unit normal vector using shift vector is

$$n^\mu = \left(\frac{1}{\alpha}, -\frac{\beta^i}{\alpha}\right) \tag{2.20}$$

Next step is choosing shape of time slice. There's no preferred slice of spacetime but there is better choice by experience. Having bad behaviour while simulation is evolving, first example is geodesic slicing. When lapse function and shift vectors are

$$\alpha = 1,\ \beta^i = 0 \tag{2.21}$$

At this situation, normal observer has vanishing four acceleration and its world line is correspond to freely falling observer's. However geodesic slicing induce singularity because extrinsic curvature K_{ij} which will be introduced later, grows exponentially.

So other choice is necessary avoiding such a singularity problem. Constrained extrinsic curvature tensor is able to avoid singularity(Smarr and York 1978) as following conditions.

$$K = 0,\ \partial_t K = 0 \tag{2.22}$$

Where K is trace of K_{ij}. One more thing, harmonic slicing is also well known gauge choice. From harmonic coordinate condition,

$$\nabla^2 x^\mu = 0 \tag{2.23}$$

The harmonic coordinate can be rewritten with respect to 3+1 splitting. Especially, the general formulation for lapse function is (Bona et al. 1995)

$$\partial_t \alpha = -\alpha^2 f(\alpha) K \tag{2.24}$$

If $f(\alpha) = 1$, it is called harmonic slicing. Note that the most popular gauge choice at recent work in numerical relativity is 1+log slicing, if $f(\alpha) = 2/\alpha$ due to strong singularity avoidance.

2.1.3 Einstein field equation

It's time to look at 3+1 decomposition anatomy for Einstein's field equation. Metric field of four dimensional spacetime is decomposed into spatial metric or three metric γ_{ij} and combination of lapse function α and shift vector β^i.

$$g_{\mu\nu} dx^\mu dx^\nu = -\alpha^2 dt^2 + \gamma_{ij} \left(dx^i + \beta^i dt\right) \left(dx^j + \beta^j dt\right) \tag{2.25}$$

Spatial metric is literally spatial so contraction with normal vector is vanished.

$$\gamma_{\mu\nu} n^\mu = 0 \tag{2.26}$$

Mixed index spatial metric is projection operator onto hypersurface, that is

$$\gamma^\mu_\nu = \delta^\mu_\nu + n^\mu n_\nu \tag{2.27}$$

By using spatial projection operator and unit normal vector, Einstein's field equation $R^{\mu\nu} + (1/2) g^{\mu\nu} R = 8\pi T^{\mu\nu}$ is projected along the normal vector, onto hypersurface or

by both of them. The field equation shows two categories of differential equation. The first part is

$$\mathcal{L}_m K_{ij} = -D_i D_j \alpha + \alpha \left(R_{ij} + K K_{ij} - 2K_{ik} K^k_j + 4\pi \left[(S - H)\, \gamma_{ij} - 2S_{ij} \right] \right) \tag{2.28}$$

This equation implies evolution of the spacetime. Ths spacetime is not freely chosen but solution of the constraint equations and those are second part of the field equation.

$$\text{(i)}\; R + K^2 - K_{ij} K^{ij} = 16\pi H \tag{2.29}$$

$$\text{(ii)}\; D_j K^j_i - D_i K = 8\pi P_i \tag{2.30}$$

For hamiltonian H and momentum P_i, both of equation gives how simulation is accurate. In theoretical speaking, L2 norm of both constraints should be 0.

2.2 Relativistic hydrodynamics

Before proceeding to dynamic equations, matter specification is necessary. Matter of the neutron star is usually described by perfect fluid which has no viscosity and thermal transport. Also, its thermal kinetic energy is fairly small comparing to rest mass energy. Employing those hypothesis, hydrodynamic equations in this chapter are valid when the matter is perfect fluid obeying cold equation of state. After that, general relativistic hydrodynamic equations will be introduced. Fluid particles are not "test particles" which do not induce curvature by itself. So, force balance equation, such as euler equation, need to deal with curvature coming from fluid particle to become general relativistic version.

2.2.1 Fluid model

Though it spoils physical reality of neutron star, many approximations are employed. Each approximation is based on thermodynamic behaviour of fluid particle and it dramatically simplifies the system to solve. Starting point is perfect fluid. It is sometimes described as ideal gas with similarity but those are totally different. More precisely, it can be thinking as 'good part of' ideal gas. Perfect fluid employ two main hypothesis

in zero-order approximation of Maxwell-Boltzmann distribution(see Rezzolla and Zanotti 2013, section 2.2.5). Higher order terms contribute thermal conductivity, shear and bulk property and so on. To remove those, it assumes that

(i) $l_{\mathrm{m}} << L$

(ii) Local Thermodynamic Equilibrium

The first assumption implies colliding very much because mean free path l_m is much smaller than characteristic length L. Frequent collision makes thermal equilibrium in time scale l_m/v, where v is characteristic velocity of system, which is equivalent to the second assumption. By them, perfect fluid is able to have well known properties such that no viscosity, no thermal transport and isotropic pressure. In relativistic manner, matter field consist of perfect fluid is following.

$$T^{\nu}_{\mu} = eu_{\mu}u^{\nu} + ph^{\nu}_{\mu} \tag{2.31}$$

e is energy density, p is pressure and $h^{\nu}_{\mu} = \delta^{\nu}_{\mu} + u_{\mu}u^{\nu}$ that is normal to fluid four velocity u^{μ}. This formulation shows isotropic pressure more intuitively. Also, following is usually used.

$$T^{\mu\nu} = (e+p)\, u^{\mu}u^{\nu} + pg^{\mu\nu} \tag{2.32}$$

When normal observer measure energy, momentum and stress of matter field, those need contraction along four velocity of the observer, n^{μ}. The energy, momentum and stress of matter with respect to normal observer are

$$H = T^{\mu\nu}n_{\mu}n_{\nu} \tag{2.33}$$

$$P_i = T^{\mu\nu}n_{\mu}\gamma_{\nu i} \tag{2.34}$$

$$S_{ij} = T^{\mu\nu}\gamma_{\mu i}\gamma_{\mu j} \tag{2.35}$$

Where γ_{ij} is three metric and it also working as projection operator from four dimensional manifold to three dimensional one. On the other hand, internal energy ϵ in closed system is

$$d\epsilon = Tds - pd\left(\frac{1}{\rho}\right) \tag{2.36}$$

by first law of thermodynamics(T is temperature, s is entropy and ρ is rest mass density). This principle will help to prove that perfect fluid is intrinsically adiabatic, i.e.

$$u^{\mu}\nabla_{\mu}s = 0 \tag{2.37}$$

at later section.

Simple model of neutron star do not possess realistic micro-physics such as nuclear interaction but it mediately contributes to gravitation via equation of state. As mentioned before, energy density ignores thermal contribution because thermal kinetic energy is much smaller than rest mass energy. This kind of equation of state is called cold equation of state. Hot equation of state, on the other hand, deal with thermal interaction and evolution. In this case thermal transport become important, which implies that higher order term in ideal gas need to be added to perfect fluid - no more perfect fluid. Limited in cold equation of state, relationship among hydrodynamic variables assume polytropic process(Horedt 2004).

$$C = \frac{dQ}{dT} = const. \tag{2.38}$$

According to relation, polytropic process assume specific heat is constant. In general, specific heat C is function of state variable and only special cases give some value or 'status'. For example, specific heat of adiabatic process is 0, and isothermal process gives ∞. From the polytropic process, it is possible to get simplified equation of state so called polytropic equation state. Perfect fluid delivers same equation of state for ideal gas so, heat is described as

$$dQ = cdT \tag{2.39}$$

$$= c_v dT - (c_p - c_v)\, T\frac{d\rho}{\rho} \tag{2.40}$$

This equation implies that

$$\frac{dT}{T} = \frac{c_p - c_v}{c_v - c}\frac{d\rho}{\rho} \tag{2.41}$$

By ideal gas equation state $P = \rho RT/\mu$, power law of T, ρ becomes P, ρ. That is

$$P = K\rho^{\Gamma} \tag{2.42}$$

where Γ is $(c_p - c)\,/\,(c_v - c)$, polytropic exponent. For adiabatic process, $c = 0$ gives well known parameter, adiabatic index.

$$\Gamma = \frac{c_p}{c_v} = \gamma \tag{2.43}$$

2.2.2 Fluid velocity on different perspective

As mentioned in previous chapter, there is no preferred observer in general relativity but we may choose comfortable one depending on physical system. Usually, eulerian(or normal) observer whose four velocity is normal vector to spacelike hypersurface and static eulerian(or coordinate) observer whose world line is world line of spatial constant, $x^i = const$. If there is fluid particle which has four velocity u^μ, each observer measure it differently and the each velocities with respect to observers have special relation. From the figure, fluid four velocity u^μ is change of four position in fluid proper

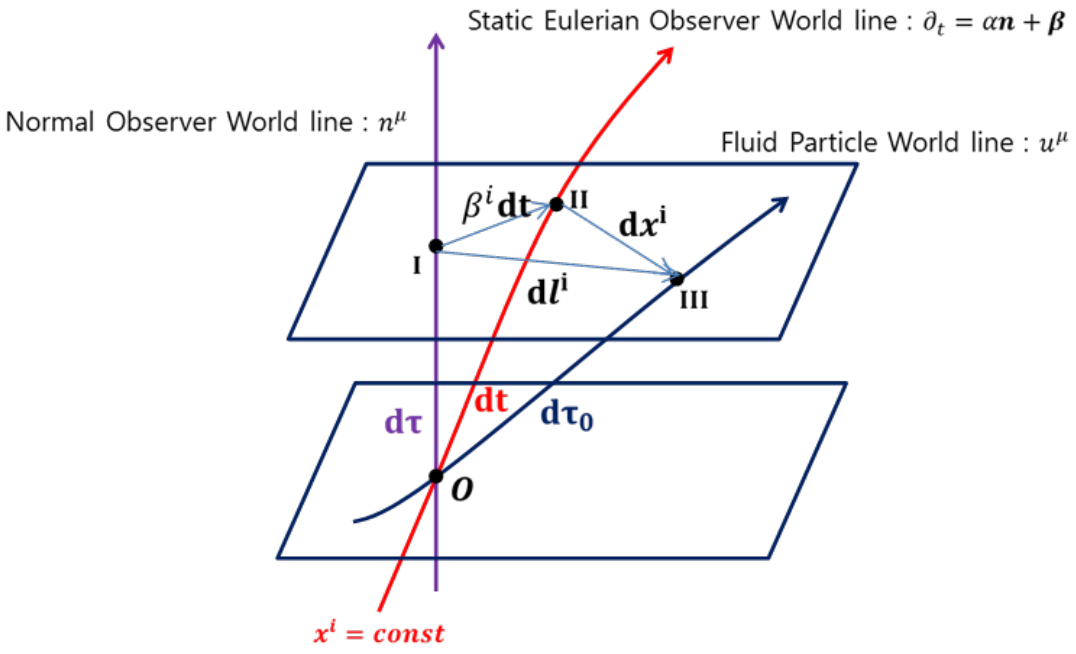

Figure 2.5: Fluid four velocity on different perspective.

time, τ_0. For fluid three velocity, spatial projection of world line of coordinate observer is $x^i = const$, 'spatial change' can be measured by position difference between coordi-

nate observer and fluid particle. The spatial part of fluid four velocity is

$$u^i = \frac{dx^i}{d\tau_0} \tag{2.44}$$

On the other hand, fluid three velocity with respect to coordinate observer is spatial difference in observer's proper time, dt. This called coordinate velocity.

$$\bar{v}^i = \frac{dx^i}{dt} \tag{2.45}$$

$$= \frac{u^i}{u^t} \tag{2.46}$$

u^t is $dt/d\tau_0$, which can think as 'time velocity' relative to fluid particle. For normal observer moving with four velocity n^μ, fluid three velocity measured by the observer is spatial change dl^i in normal observer's proper time $d\tau$.

$$v^i = \frac{dl^i}{d\tau} \tag{2.47}$$

According to triangle identity, dl^i is described as

$$\mathbf{u}\ d\tau_0 = d\mathbf{l} + \mathbf{n}\ d\tau \tag{2.48}$$

Applying projection along n^μ, spatial part dl^i is vanished. Also, fluid proper time is lorentz contracted by normal observer's proper time, $d\tau = W d\tau_0$. Then,

$$-n^\mu u_\mu = W \tag{2.49}$$

Now, employing relation $\alpha dt = d\tau$ coming from ADM 3+1 formalism, lorentz factor W is multiplication of lapse function and time velocity. Differentiating triangle identity with fluid proper time, fluid four velocity is decomposed into four velocity of normal observer and spatial part of fluid four velocity of the observer's perspective.

$$u^\mu = W\left(n^\mu + v^\mu\right) \tag{2.50}$$

Of course, v^μ has no normal component so $v^\mu n_\mu = 0$. Next looking at just hypersurface in the figure, another triangle appears.

$$dl^i = \beta^i dt + dx^i \tag{2.51}$$

The second triangle show that(differentiating with respect to $d\tau$)

$$v^i = \frac{\bar{v}^i}{\alpha} + \frac{\beta^i}{\alpha} \tag{2.52}$$

$$= \frac{u^i}{\alpha u^t} + \frac{\beta^i}{\alpha} \tag{2.53}$$

This velocity shape is employed by one of relativistic hydro code called Valencia formulation. From now on, spatial part of fluid four velocity relative to normal observer will be called as valencia velocity. It delivers meaning that fluid four velocity in two different perspective and each velocity is connected by coordinate variables.

2.2.3 Fundamental equations

From energy momentum conservation of matter field, various hydrodynamic equations can be obtained. For perfect fluid, energy momentum conservation is

$$\nabla_\mu T^\mu_\nu = \nabla_\mu \left[(e+p) u^\mu u_\nu + p\delta^\mu_\nu \right] \tag{2.54}$$

$$= (e+p) \nabla_\mu (u^\mu u_\nu) + u^\mu u_\nu \nabla_\mu (e+p) + \nabla_\mu p \tag{2.55}$$

As ADM 3+1 formalism split four dimensional quantities into space and time, energy momentum conservation equation will be decomposed into two parts, one is moving along fluid four velocity and the other is orthogonal to fluid four velocity. Contraction with u^μ implies that projection to fluid four velocity.

$$u^\nu \nabla_\mu T^\mu_\nu = -(e+p) \nabla_\mu u^\mu - u^\mu \nabla_\mu e \tag{2.56}$$

$$= 0 \tag{2.57}$$

Density current $J^\mu = \rho u^\mu$ is also conserved because there's no mass lose or gain. So,

$$\nabla_\mu (\rho u^\mu) = 0 \tag{2.58}$$

By rest mass conservation, new identity such that

$$\nabla_\mu u^\mu = -\frac{1}{\rho} u^\mu \nabla_\mu \rho \tag{2.59}$$

is appeared. Moreover, thermodynamic relation show that specific enthalpy h is equivalent to $(e+p)/\rho$. Therefore,

$$u^\mu \nabla_\mu e - h u^\mu \nabla_\mu \rho = 0 \tag{2.60}$$

It is relativistic energy conservation equation. Part of the second term $-u^\mu \nabla_\mu \rho$ measures how much fluid particle expand along the fluid line, which is called expansion parameter. When the fluid particle is incompressible, the expansion parameter is vanished. According to first law of thermodynamics, $de = hd\rho + \rho T ds$, relativistic energy conservation prove that intrinsic nature of perfect fluid is adiabatic as mentioned at section 2.2.1.

On the other hand, projection along orthogonal to fluid four velocity delivers

$$h^\nu_\lambda \nabla_\mu T^\mu_\nu = \left(\delta^\nu_\lambda + u^\nu u_\lambda\right) \nabla_\mu \left[(e+p)\, u^\mu u_\nu + p\delta^\mu_\nu\right] \tag{2.61}$$

where $h^\nu_\mu = \delta^\nu_\mu + u^\mu u_\nu$ is projection operator. After few algebra, it reveals equation of motion.

$$(e+p)\, u^\mu \nabla_\mu u_\lambda + \nabla_\lambda p + u_\lambda u^\nu \nabla_\nu p = 0 \tag{2.62}$$

It can be rewritten as

$$\rho h a_\lambda + h^\nu_\lambda \nabla_\nu p = 0 \tag{2.63}$$

This equation represents relativistic euler equation which implies force balance in curved spacetime. According to relativistic euler equation, fluid particle is not on the geodesic world line in general. When pressure is homogeneous, fluid world line is correspond to geodesics. If killing symmetry is imposed in the system, something conserved exist. This fact connect to Bernoulli's equation, another energy conservation equation along the fluid line.

So far, fluid do not care about flow configuration. From now, fluid particle show special character by imposing irrotational flow. Vorticity is attributed to rotational configuration of the fluid particle, it will be treated in detail later. Different from Newtonian hydrodynamics, vorticity is defined by not only fluid velocity but also matter field. The vorticity tensor is

$$\Omega_{\mu\nu} = \nabla_\nu \left(h u_\mu\right) - \nabla_\mu \left(h u_\nu\right) \tag{2.64}$$

The vorticity tensor become 0 when flow is irrotational. Vorticity of fluid world line is contraction between the two form vorticity and fluid four velocity.

$$\Omega_{\mu\nu}u^{\nu} = hu^{\nu}\nabla_{\nu}u_{\mu} + u_{\mu}u^{\nu}\nabla_{\nu}h + \nabla_{\mu}h \tag{2.65}$$

Due to euler equation, $ha_{\mu} = -1/\rho\ h^{\nu}_{\mu}\nabla_{\nu}p$, the equation above converts to following.

$$\Omega_{\mu\nu}u^{\nu} = \nabla_{\mu}h - \frac{1}{\rho}\nabla_{\mu}p + u_{\mu}u^{\nu}\left(\nabla_{\mu}h - \frac{1}{\rho}\nabla_{\mu}p\right) \tag{2.66}$$

First law of thermodynamics tells $\nabla_{\mu}h - (1/\rho)\nabla_{\mu}p = T\nabla_{\mu}s$ and perfect fluid is adiabatic, i.e., $u^{\nu}\nabla_{\nu}s = 0$. Therefore,

$$\Omega_{\mu\nu}u^{\nu} = T\nabla_{\mu}s \tag{2.67}$$

It is called Carter-Lichnerowicz equation of motion(Lichnerowicz 1967, Cater and Gaffet 1988). The equation relates flow configuration and state variable limited in perfect fluid. For example, irrotational perfect fluid is isentropic no matter what temperature is. For neutron star binary system, inspiral phase is characterized by irrotational flow. Therefore inspiral neutron star binary is in isentropic process(again, we assume the fluid is perfect) before the stars are merging.

2.2.4 Flow configurations

Though fluid dynamics suggest nice equation of motion, it is hard to get exact solution due to its non-linear and complex behaviour. However killing vector which deliver symmetry of the system dramatically simplify physical situation. One of fluid flow containing such a symmetry is stationary flow. Literally, stationary flow has time symmetry so its physics is invariant with respect to time evolution. Because the 'time' is depending on observer in the system, time at this subsection means coordinate time that is proper time ∂_t for observer on $x^i = const.$ worldline. Before proceeding to stationary flow, let's see special property of Killing vector with arbitrary symmetry. Gravitational field of system that is represented by metric is invariant if it is Lie dragged.

$$\mathcal{L}_{\xi}g_{\mu\nu} = 0 \tag{2.68}$$

where ξ is Killing vector. It becomes following.

$$\begin{aligned} \mathcal{L}_\xi g_{\mu\nu} &= \xi^\alpha \frac{\partial g_{\mu\nu}}{\partial x^\alpha} + g_{\alpha\mu}\frac{\partial \xi^\alpha}{\partial x^\nu} + g_{\alpha\nu}\frac{\partial \xi^\alpha}{\partial x^\mu} && (2.69) \\ &= \nabla_\nu \xi_\mu + \nabla_\mu \xi_\nu && (2.70) \end{aligned}$$

From relativistic euler equation, imposing conditions such that

$$\text{(i) } dp = \rho dh - \rho T ds$$

$$\text{(ii) } \nabla_\nu \xi_\mu + \nabla_\mu \xi_\nu = 0$$

$$\text{(iii) } \mathcal{L}_\xi q = 0$$

where q is hydro variable like energy density e or pressure p. The third condition states hydro variables share same symmetry as field variable on spacetime. Then relativistic Bernoulli's equation is revealed as mentioned at the previous subsection.

$$\begin{aligned} u^\mu \nabla_\mu \left(h u_\nu \xi^\nu\right) &= 0 && (2.71) \\ &= \mathcal{L}_u \left(h u_\nu \xi^\nu\right) && (2.72) \end{aligned}$$

Enthalpy current along Killing vector is conserved and it is called injection energy. Going back to stationary flow, Killing vector field is $\boldsymbol{\xi} = (1, 0, 0, 0)$.

$$h u_\nu \xi^\nu = h u_t \tag{2.73}$$

Therefore, 1 form enthalpy current hu_t is conserved quantity in stationary spacetime(also matter field is). Another example is irrotational flow. Newtonian counterpart is measured by curl of velocity but in relativistic hydrodynamics, it is defined by not only velocity but also matter contribution.

$$\begin{aligned} \Omega_{\mu\nu} &= \partial_\nu \left(h u_\mu\right) - \partial_\mu \left(h u_\nu\right) && (2.74) \\ &= \nabla_\nu \left(h u_\mu\right) - \nabla_\mu \left(h u_\nu\right) && (2.75) \end{aligned}$$

Due to $\Gamma^\alpha_{(\beta\gamma)} = 0$, it seems partial derivative is same to covariant derivative. This 2 form is vorticity tensor, which is different to canonical vorticity. Let's looking definition of

vorticity precisely. Partial derivative terms are same to exterior derivative of enthalpy current so, fluid vorticity can be interpreted as boundary of the enthalpy current.

$$\Omega_{\mu\nu} = \mathbf{d}\left(hu\right)_{\mu\nu}. \tag{2.76}$$

When vorticity is vanished, enthalpy current is gradient of some scalar field.

$$hu_{\mu} = \nabla_{\mu}\Phi \tag{2.77}$$

This is velocity potential and rest mass conservation $\nabla_{\mu}\left(\rho u^{\mu}\right) = 0$ build velocity potential equation.

$$\nabla_{\mu}\left(\frac{\rho}{h}\nabla^{\mu}\Phi\right) = 0 \tag{2.78}$$

It can be solved by elliptic solver or approximated by constant spatial velocity which will be explained at next subsection.

Chapter 3

Numerical methods

To calculate relativistic behaviour, many useful codes are developed and the code called Einstein toolkit(Loffler et al 2011) is one of available codes. Einstein toolkit is based on `Cactus` framework and it consists of modules called thorn. Though each thorn is written by different language and variable statements but they can implement, inherit via flesh code. This chapter briefly explain basic numerical structure for differentiation and integration and then, introduce thorns which are frequently utilized for the study.

3.1 Finite difference method

General relativity intrinsically possesses family of partial differential equations. For second order partial differential equations, they are demonstrated by some categories. A general type is

$$A\partial_{xx}u + B\partial_{xy}u + C\partial_{yy}u + \cdots = 0 \tag{3.1}$$

where u is arbitrary function. By coefficients A, B and C,

(i) $B^2 - 4AC < 0$: Elliptic equation

(ii) $B^2 - 4AC = 0$: Parabolic equation

(iii) $B^2 - 4AC > 0$: Hyperbolic equation

First, elliptic equation delivers smooth solution and constraint equation is one of example. Parabolic equation is numerically difficult equation and hyperbolic equation depends on situation. It sometimes show discontinuity and evolution equation of hydrodynamics is typical example. Differential equations in numerical relativity is composed of scalar, vector and tensor fields variables and its calculations are carrying out in grid domain. Size of grid cell is related to simulation accuracy and running time. Fine grids ensure that precise simulation but it takes too much time. It means that optimization is necessary. The structure of grid domain is depending on problem because part of the domain where we are interesting is different. For example, orbital evolution of neutron star binary simulation need to resolve stars. If the interest is star collision, central grids should have high resolution. In fact, both orbital evolution and merging are important in compact binary simulation, so the finest grid domain covers stars and central region.

In grid nature, finite difference method describes approximated derivatives by linear combination of values at the grid points nearby. According to Taylor series,

$$U\left(x\right)=\sum_{n=0}^{\infty}\frac{\left(x-x_i\right)^n}{n!}\frac{\partial^n U}{\partial x^n} \tag{3.2}$$

the first derivative means 'slope' or 'how much function changes' while x is changing. From the derivatives which is chosen at certain points, estimating next, previous or central point value is possible as Figure 3.1.1. In other words, forward, backward and central finite difference methods provide first derivative followings.

$$\text{central}: \quad \frac{\partial U}{\partial x}\sim\frac{U_{i+1}-U_{i-1}}{2\Delta x} \tag{3.3}$$

$$\text{backward}: \quad \frac{\partial U}{\partial x}\sim\frac{U_{i+2}-U_{i+1}}{\Delta x} \tag{3.4}$$

$$\text{forward}: \quad \frac{\partial U}{\partial x}\sim\frac{U_{i+1}-U_{i}}{\Delta x} \tag{3.5}$$

Comparing truncation error with each finite difference method, central one shows better accuracy in same order of approximation. Therefore, central finite method is implemented in the source code. When the problem expands from 1D to 2D, the second

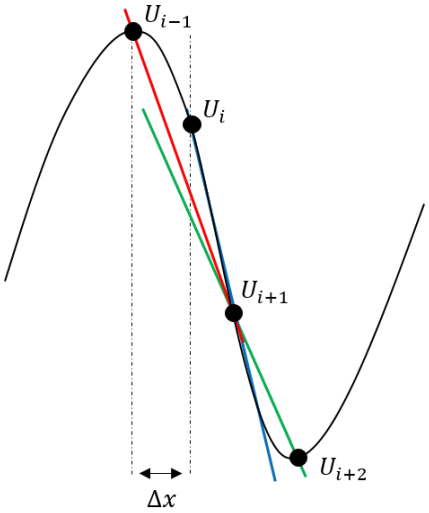

Figure 3.1: Three finite difference methods. Red, green and blue lines represents central, backward and forward finite difference method respectively.

order central finite difference given grid structure as Figure 3.1.2 as

$$\partial_x u_{j,k} = \frac{u_{j+1,k} - u_{j-1,k}}{2\delta h_x} \tag{3.6}$$

$$\partial_y u_{j,k} = \frac{u_{j,k+1} - u_{j,k-1}}{2\delta h_y} \tag{3.7}$$

where $\delta h_x = x_{j+1} - x_j$ and $\delta h_y = y_{k+1} - y_k$. Finite difference method typically employ at least fourth order approximation due to simulation accuracy. The fourth order is following.

$$\partial_x u_{j,k} = \frac{-u_{j+2,k} + 8u_{j+1,k} - 8u_{j-1,k} + u_{j-2,k}}{12\delta h_x} \tag{3.8}$$

$$\partial_y u_{j,k} = \frac{-u_{j,k+2} + 8u_{j,k+1} - 8u_{j,k-1} + u_{j,k-2}}{12\delta h_y} \tag{3.9}$$

From the finite difference method formulation, grid points need to know value of neighbourhood. For first derivative of the points, higher order accuracy requires more points and a required number of points is called stencil. Fourth order derivative example above has stencil size 2. In relativistic simulation, it is usually calculated by parallel computing which utilize multi cores because general relativity contains heavy differential equations. Each CPU shares grid domain and interacts each other via network.

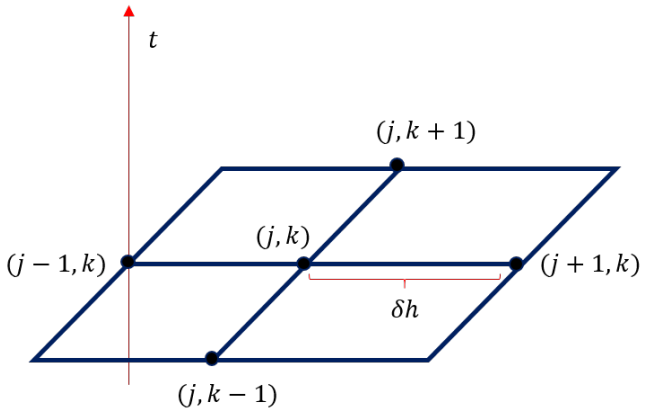

Figure 3.2: Simple grid structure. δh is $x_{j+1} - x_j$. Assume that variation in y direction also gives δh. That is $\delta h_x = \delta h_y = \delta h$

Like derivative which requires data points nearby, it can be problematic when stencil touch outer grid domain where other CPU is calculating. Boundary domain between blue and red square stores information of part of outer grid points and it is called ghost zone. If simulation does higher order finite difference method, proper size of ghost zone is necessary.

3.2 Time integration

As mentioned at previous section, evolution equation is hyperbolic so it requires different scheme to solve it. Time integration method called Runge-Kutta method employing Method of Line(hereafter MoL) is frequently used in this study. Partial differential equation has many variables but MoL converts multi variable system to ordinary differential equation. For general form,

$$\frac{du}{dt} = L\left(u_i^n\right) \tag{3.10}$$

Here L denotes differential operator. L and discretized variable u_i^n do not depend on time so Equation 3.2.1 become ordinary differential equation. Then Runge-Kutta can

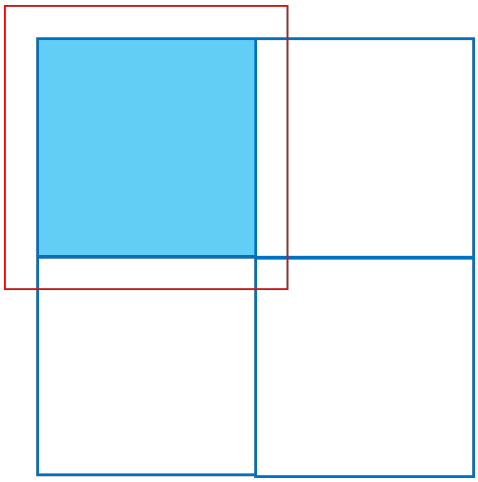

Figure 3.3: Example of root domain and ghost zone. The largest blue square is whole physical domain and it is divided by 4 local regions. Each local region is calculated by each CPU and data on domain boundary or its nearby share information via ghost zone, intermediate region between blue and red square.

deal with equations. For the fourth order method,

$$k_1 = u(t_n, x_n) \tag{3.11}$$

$$k_2 = u(t_n + \alpha_1 \Delta t, x_n + \beta_1 k_1 \Delta t) \tag{3.12}$$

$$k_3 = u(t_n + \alpha_2 \Delta t, x_n + \beta_2 k_2 \Delta t) \tag{3.13}$$

$$k_4 = u(t_n + \alpha_3 \Delta t, x_n + \beta_3 k_3 \Delta t) \tag{3.14}$$

k_1 is original term multiplying just Δt and the others are higher order correction term. That means factor from k_2 to k_4 modifies path of function u with respect to coordinate time t. Coefficients α_i, β_i are determined by Taylor series expansion such that

$$u_{n+1} = u_n + \dot{u}_n \Delta t + \frac{1}{2} \ddot{u}_n (\Delta t)^2 + \dots \tag{3.15}$$

until fourth order. Final form of time integrated is

$$x_{n+1} = x_n + (k_1 + 2k_2 + 2k_3 + k_4) \frac{\Delta t}{6} \tag{3.16}$$

3.3 `Cactus` code

Einstein toolkit contains many codes and each code is written by different languages or different variable statements. Nevertheless the codes can interact among them through `Cactus` framework flesh, this is one of key works of it. Among the codes, the most important function is building grid structure and it is provided by `Carpet`(see Schnetter et al 2004 for more detail). It is adaptive mesh refinement driver so it supports simulation that covers physics in different length scales. For example, moving stars need following grid with high level of resolution but atmosphere region does not need it. `Kranc` reconstruct computer code from the mathematical description and `Simulation Factory` provides interface operation like job running. Those four function is core technologies of Einstein toolkit.

Einstein toolkit contains initial data generator for black hole binary employing two puncture method but not neutron star binary. We rely on `LORENE` code for 'analytic' solution though it deals with quasi circular orbit only. However, it is able to provide kind of standard or tendency of initial data and evolution. That means we can compare the results from the strategy of us. `LORENE` generates initial data file and Einstein toolkit evolve it. Geometrical units of `LORENE` and Einstein toolkit is different, so there are thorn `Meudon` series that interpret units from `LORENE` to `Cactus`.

Focus of this paper is neutron star binary in eccentric orbit but there is no code for initial data calculation in eccentric orbit. By using `TOVSolver`, building up the initial data is possible but is not accurate. `TOVSolver` is a thorn to construct initial data for single or multi TOV stars. It solves ordinary differential equation for pressure P, gravitational mass m and metric potential in terms of distance r via Runge-Kutta method. Then it is transformed to isotropic coordinate and carrying out three dimension interpolation. Setting a number of TOV star as two with arbitrary separation, it becomes binary system. Hydro variables from `TOVSolver` transfer to thorn `Hydrobase`, which reorganize the variable to make them implemented by another codes. That codes typically contribute to evolution, for example `GRHydro` or `EosOmni`. `GRHydro` is another form of `Whisky`(Baiotti et al 2005) code, which solves eigen value problems. `EosOmni`

cares about evolution of equation of state, generally employing ideal equation of state evolution. Likewise `Admbase` also deal with same problems limited in spacetime variable such as lapse function, shift vector or metric field. Finally thorn `IO` provide outputs of simulation. Thorns are characterized by parameter files. Some thorns are automatically activated if required thorns are registered.

Chapter 4

Single TOV star

This chapter is going to provide basic notion for TOV star, the simplest theoretical approach describing neutron star. Though this is not a realistic stellar model but it gives good insight with respect to gravitation from compact star which have finite size. It covers original solution, static, stationary TOV star and treats boosted star in next section.

4.1 Static and stationary TOV star

TOV star is a simple structure of relativistic star such as white dwarf or neutron star, postulated by Tolman, Oppenheimer and Volkoff for the first time. Though the stars have special micro-physics, TOV star model focus on gravitation of the matter field mostly. Special aspects of TOV star are summarized by following two statements.

(i) TOV star is spherical symmetric.

(ii) Fluid matter is barotropic.

The first statement, spherical symmetric star ensure that static and stationary state by Birkhoff's theorem. So projection of fluid four velocity onto hypersurface is vanished.

$$u^{\mu}_{\mathrm{TOV}} = \left(u^{t}, 0, 0, 0\right) \tag{4.1}$$

Moreover, fluid keeps ideal equation of state without viscosity. Though ideal gas shows that rest mass density and pressure has relation with temperature, barotropic fluid can ignore thermal contribution to dynamics. That is reason why the second statements is necessary. In short, static and stationary TOV star is derived from Einstein's field eqution $R^{\mu\nu} + (1/2)\, g^{\mu\nu} R = 8\pi T^{\mu\nu}$ which deal with gravitation part of the star and energy momentum conservation $\nabla_\mu T^{\mu\nu} = 0$. Metric field for neutron star is similar to Schwarzschild metric. One thing different is finite size so exterior region of the neutron star is exactly correspond to static black hole solution interior region isn't.

$$g_{\mu\nu} dx^\mu dx^\nu = -e^{2\psi} dt^2 + \left(1 - \frac{2m}{r}\right)^{-1} dr^2 + r^2 \left(d\theta^2 + \sin^2\theta d\phi^2\right) \tag{4.2}$$

With spherical symmetry, ψ is mteric potential and m is gravitational mass confined

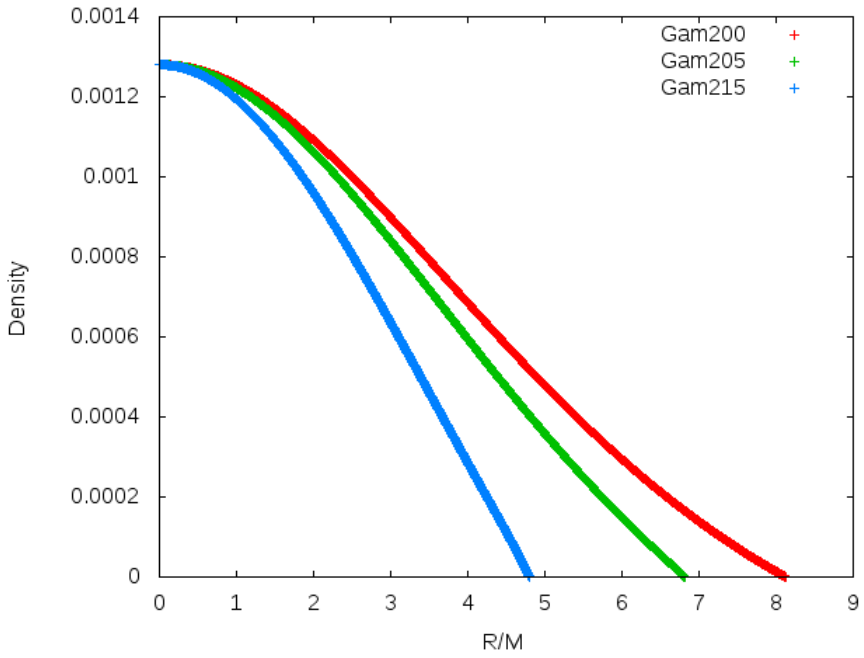

Figure 4.1: Initial rest mass density profile for static and stationary neutron star. Higher polyropic exponent fluid is closer to incompressible fluid.

in radius r. If $r = R$ where R is radius of star, m is mass of neutron star M. Spherical symmetric metric, perfect fluid containing polytropic process govern physical character

of isolated neutron star.

$$\frac{dm}{dr} = 4\pi r^2 e = 4\pi r^2 \rho\,(1+\epsilon) \tag{4.3}$$

$$\frac{dp}{dr} = -\,(e+p)\,\frac{d\psi}{dr} = -\,(e+p)\,\frac{m+4\pi r^3 p}{r\,(r-2m)} \tag{4.4}$$

$$\frac{d\psi}{dr} = \frac{m+4\pi r^3 p}{r\,(r-2m)} \tag{4.5}$$

An isotropic metric also can describe neutron star, which is sphere nested coordinate. It takes the form as

$$g_{\mu\nu}dx^\mu dx^\nu = -e^{2\psi} + e^{2\chi}\left(d\bar{r}^2 + \bar{r}^2 d\Omega^2\right) \tag{4.6}$$

Here $\bar{r}$ denotes isotropic radius. Though formulation of the metric field is different but they describe same thing. Matching both of them, it apparently shows that

$$r^2 = e^{2\chi}\bar{r}^2 \tag{4.7}$$

$$\left(1-\frac{2m}{r}\right)dr^2 = e^{2\chi}d\bar{r}^2 \tag{4.8}$$

Combining a pair of equations implies coordinate transformation between two metric field. The formulation is

$$e^{\psi} = \frac{\left(1-\frac{M}{2\bar{r}}\right)}{\left(1+\frac{M}{2\bar{r}}\right)} \tag{4.9}$$

$$\gamma_{ij} = \left(1+\frac{M}{2\bar{r}}\right)^4 \tag{4.10}$$

where $\gamma_{ij} = \gamma_{xx} = \gamma_{yy} = \gamma_{zz}$. In isotropic coordinate, initial profiles of static and stationary neutron star can be obtained. Figure 4.1.1 and 4.1.2 shows how polytropic exponent effect on size and profile of the star. In geometrical unit, setting $K = 100$ and $\rho = 0.00128$ for central region. In the Figures, Gam denotes polytropic exponent Γ and the number means $2, 2.05, 2.15$ respectively. As equation of state become stiff, radius and confined mass decrease. In other word, stiff equation of state requires more dense central density than soft one if they has same radius. Note that polytropic equation of state is not realistic equation of state. Realistic model implies nuclear interaction in the neutron star and such equations of state are described by piecewise polytropic equation of state(Read et al 2009).

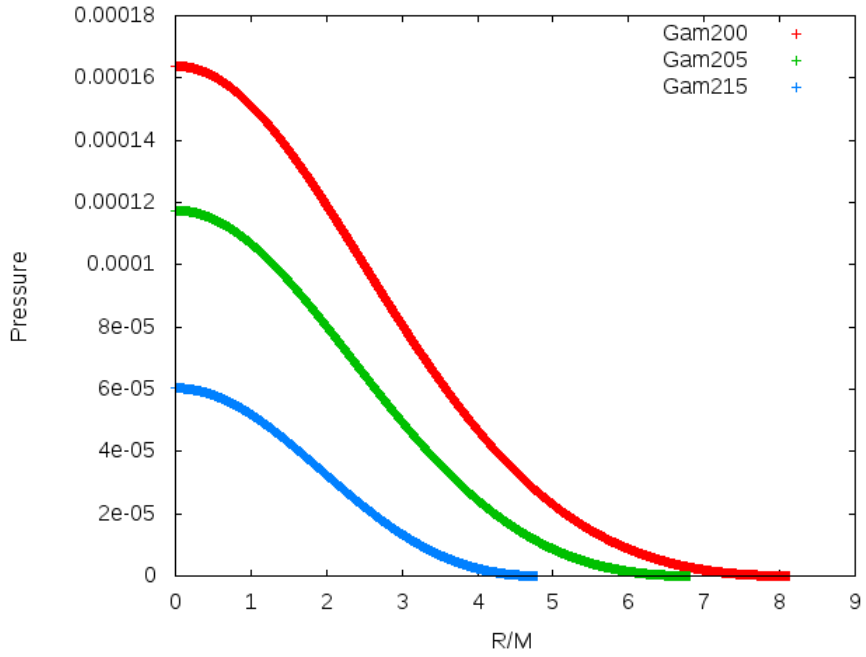

Figure 4.2: Initial pressure profile for static and stationary neutron star

4.2 Boosted TOV star

When TOV star is no more static, it shows somewhat strange behaviour. It might be coming from spherical symmetry broken which insist static and stationary solution. Boost make Lorentz contraction along boosted direction so it shows little oblate shape(Note that all of fluid particles in the neutron star have same velocity). Then relativistic euler equation also breaks down, force imbalance occurs. According to Figure 4.1.3, normalized maximum density oscillation of static TOV is stable but boosted TOV shows excited mode. If there is exact metric field describing boosted TOV star with stationarity, the density oscillation can be relived because relativistic euler equation compatible with that metric keeps stable mode. Looking more precisely, boosted TOV star possesses high frequency mode which does not occur in static TOV star. That frequency mode may come from surface vibration due to force imbalance as we mentioned.

Result from the boosted TOV star implies that artificial velocity without proper

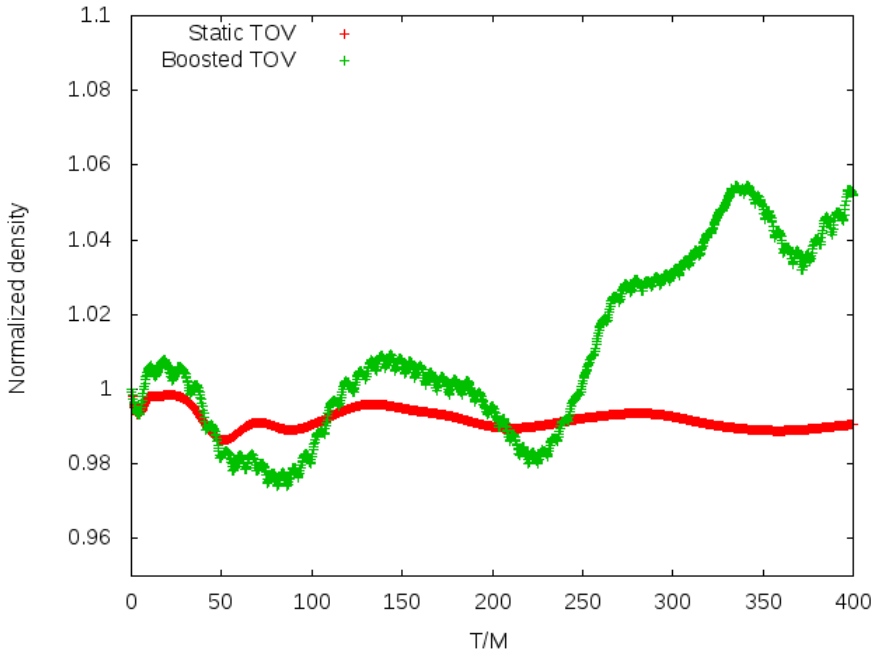

Figure 4.3: Maximum density oscillation of boosted TOV. High frequency and low frequency mode occur due to boost parameter.

treatment can deliver strange oscillation as Figure 4.2.1. It is very important conclusion because we are going to add boost to create eccentric binary. Limited in bounded system (the binary system going to merge), quasi circular orbit requires the largest angular momentum and it is obvious that such velocity spoils oscillation mode. Therefore, 'proper treatment' should be figured out to remove spurious oscillation.

Chapter 5

System consists of TOV stars

5.1 Introduction

Einstein's field equation is naturally constrained system so it needs proper initial data to evolve. For system which contains more than one relativistic star, it must solve hamiltonian and momentum constraint equations of the system. It is possible to employ reduced mass to care about multiple stars but that is Newtonian story. In Einstein gravity, it does not admit reduced mass or metric superposition of each star.

$$g_{\mu\nu} \neq g^{(1)}_{\mu\nu} + g^{(2)}_{\mu\nu} + \cdots + (1-n)\,\eta_{\mu\nu} \tag{5.1}$$

$\eta_{\mu\nu}$ means flat metric and factor $(1-n)$ is extracting overlapped background metric. Though superposed metric field is wrong, it is utilized as numerical trick when the stars are orbiting eccentric orbit and are located at far away from each other(Gold et al 2012), at least 200km. Then, constraint violation or unphysical behaviour is fairly decreased. Moreover, it is not trivial working to get initial data for eccentric orbit. `LORENE` or `SGRID` can create reliable initial data for quasi circular orbit but they can't for eccentric case. Because it is very difficult problem managing dynamical deformation from tidal field of the neutron star companion. However it certainly suggest very intriguing and distinctive physical aspect which is not able to measure in quasi circular orbit. For instance, gravitational wave shows dynamical amplitude and phase change or horizon

shape of black hole remnant may be various. Threshold mass, different rotation of remnant neutron star, every dynamical parameter limited in quasi circular orbit shall be changed.

This chapter focuses on little bit more challenging problem that neutron star binary initial data in eccentric orbit through hydro perturbation. Main point is how to assert perturbation configuration. Strong Bernoulli's theorem can provide proper guide line of the perturbation. The perturbation asserts pressure variation without density change. It will be very meaningful with respect to treating initial data problem of eccentric orbit in simple way. There are two parts to make sufficiently useful initial data. One is hydro variable and the other is gravitation. Correct metric field contributes accurate gravitation but it will be ignored. Only hydrodynamical correction is applied via pressure perturbation. We also carry out simulation employing `LORENE` initial data before proceeding to out strategy because it can give physical standard. In quasi circular orbits or near quasi circular orbits can be compared with analytic data.

5.2 Head-on collisions of TOV stars

Before handling initial data for neutron star binary, head-on collision can give good insight for potential error of boosted system. First step is construct metric field that is not a solution for constraint equation. There are two options for metric, one is superposition of isolated neutron star solution or sewing the isolated solution at the symmetry boundary. Difference between those metric configuration is whether feeling external metric field initially or not. According to Figure 5.2.1, lapse function of superposition feels external gravitation as

$$\alpha_{\mathrm{sup}} - \alpha_1 = \sqrt{1 - \frac{2M_2}{\|\mathbf{D} - \mathbf{r}\|}} - 1 \tag{5.2}$$

Here $\mathbf{D}$ is separation vector of two stars and M_2 is gravitational mass of companion. On the other hand, lapse function of maximum method cannot feel external field due to companion initially.

$$\alpha_{\mathrm{max}} - \alpha_1 = 0 \tag{5.3}$$

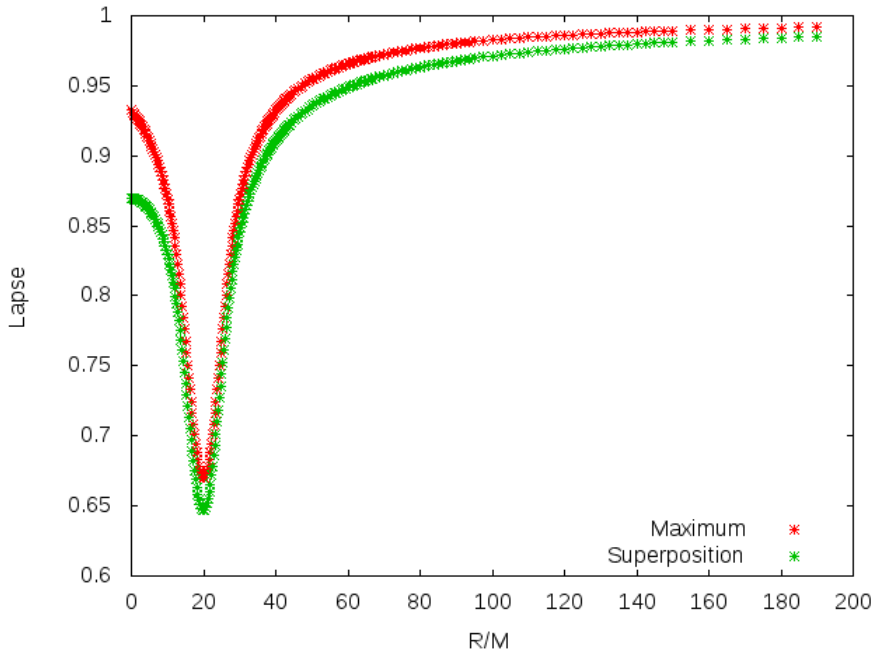

Figure 5.1: Lapse function of maximum and superposition method in 1D plot. Maximum represents sewing TOV metric at the $x = 0, y = 0$ line.

As time is evolving, lapse function of maximum method gradually feels external field. Note that both of configuration treats metric field only so stars do not 'react' for that. For example, though metric superposition can provide external field strength (no matter how it accurate), neutron stars are not deformed initially. Shift vectors or other hydro variables like rest mass density, energy density, etc are simply superposed no matter what metric combination method is.

$$\beta^i = \beta^i_1 + \beta^i_2, \;\; q = q_1 + q_2 \tag{5.4}$$

Where q represents hydro variables. Each combination method has both of weak and strong points and it's time to check how they affects time evolution of spacetime and hydro variable. The most important thing to fix is spurious oscillation of maximum density. One said reason why such a problem occur is attributed to definition of stationarity (Moldenhauer et al. 2014), but it seems to depend on approaching method. In this research, spurious oscillation come from force unbalance or spoiled irrotational

flow. Figure 5.2.2 shows central density oscillation when coordinate separation is 60km, normalized by initial central density. Relativistic euler equation states that force balance between gravitation and pressure gradient. Superposed metric is initially balanced with self gravitation so it is obvious that balance broken because of external field. This fact delivers unphysical amplitude.

Maximum metric seems to show much better evolution than superposed metric. It should do because initial configuration is based on isolated neutron star so there is no cause to trigger force unbalance. But in constraint violation perspective, simulation with maximum metric is likely to be unreliable at the boundary. Figures 5.2.3 tells that point 0 and its neighbourhood is working bad. The others points behave better than superposed metric but those two points spoils constraints violation very much. If lapse function become smooth via artificial control, decreased constraint violation is expected. If the system got boosted, another unphysical oscillation may occur as booted TOV star. Choosing maximum metric configuration will help to solve problem easier way - just thinking about boost effect on neutron star. In binary system, it is going to employ maximum metric configuration with some kinds of approximation.

5.3 Quasi circular orbit

`LORENE` utilizes multi grid domains employing spectral method. Simply speaking, it finds proper enthalpy level surface from double TOV star as initial guess via iteration. It considers deformation of star due to external gravity of companion, which is one of big differences from our strategy. Figure 5.3.1 shows that baryonic density on the xy plane. Closed curves in the neutron stars represent iso-density region and it will rotate irrotationally. `LORENE` employs different geometrical unit from `Cactus`, rescaling is necessary. For instance, polytropic equation of state is

$$p = \kappa n^{\gamma} \tag{5.5}$$

where n is scaled baryonic density. When we provide initial parameter such as central baryonice density, κ and polytropic exponent, code reads the inputs calculate initial

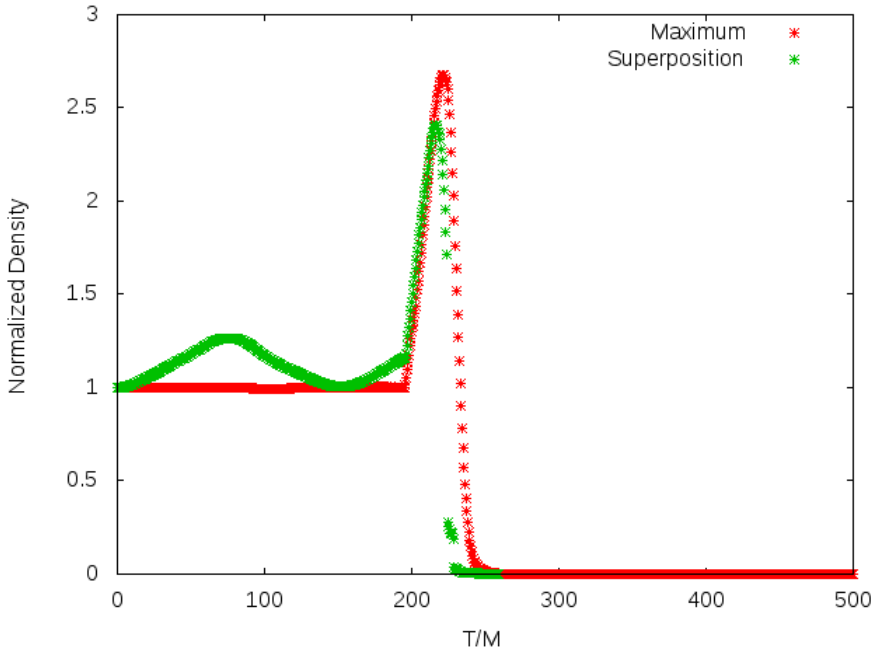

Figure 5.3: Maximum density oscillation of head-on collision in 1D plot

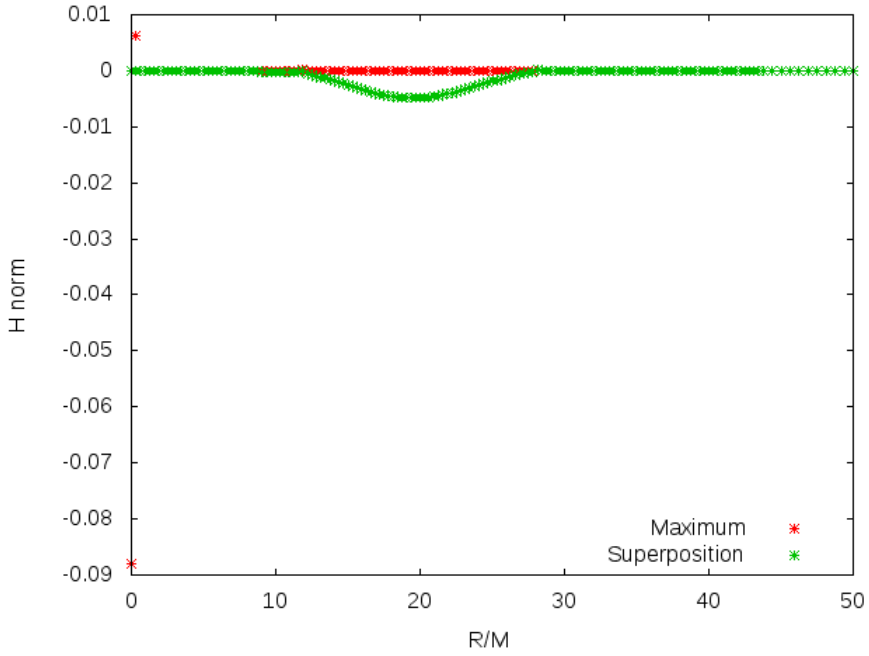

Figure 5.4: Hamiltonian constraint violation of head-on collision in 1D plot

data via iteration. We run a public initial data in `LORENE` websites. Neutron star has

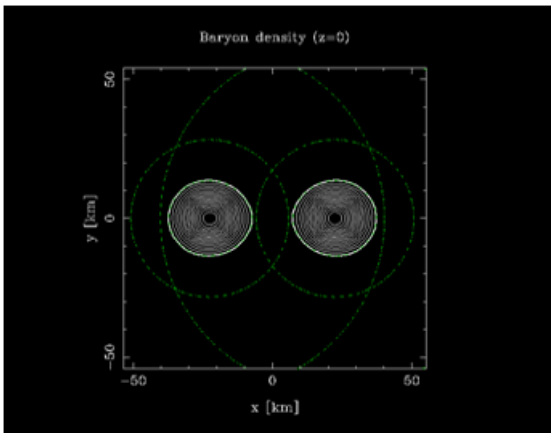

Figure 5.2: Baryonic density from the `LORENE` initial data generator. Looking precisely, neutron stars are deformed along direction of companion. The strategy of us, which will be introduced later section, cannot see initial deformation.

central density about 0.001228 in `Cactus` unit and total mass is about 1.7 solar mass. Though total mass and central density is different from the system that we are going to examine, we can see kind of tendency.

In general relativistic simulation, there is criteria whether the simulation is accurate or not. When constraint violation is fairly small (at least 10^{-6}), the simulation is reliable. However, that is the case for "analytically solved". Making initial data without solving constraint equation can deliver large error or show better constraint violation through artificial management. Therefore not only constraint violation but also another physical aspect like density oscillation or gravitational wave should be investigated.

First, let's see central density oscillation of neutron star. It gives little bit different oscillation comparing with single TOV star. That is due to tidal field of companion and velocity configuration(Of course, different density or K are also attributed to difference). Central density amplitude shows very stable evolution and at coordinate time 600 it is suddenly increasing and keeps small excitation. Gravitational wave from the `LORENE` initial data shows junk radiation which is physically wrong. This junk is able to deleted via filtering when it is time integrated. Hamiltonian constraint of the system

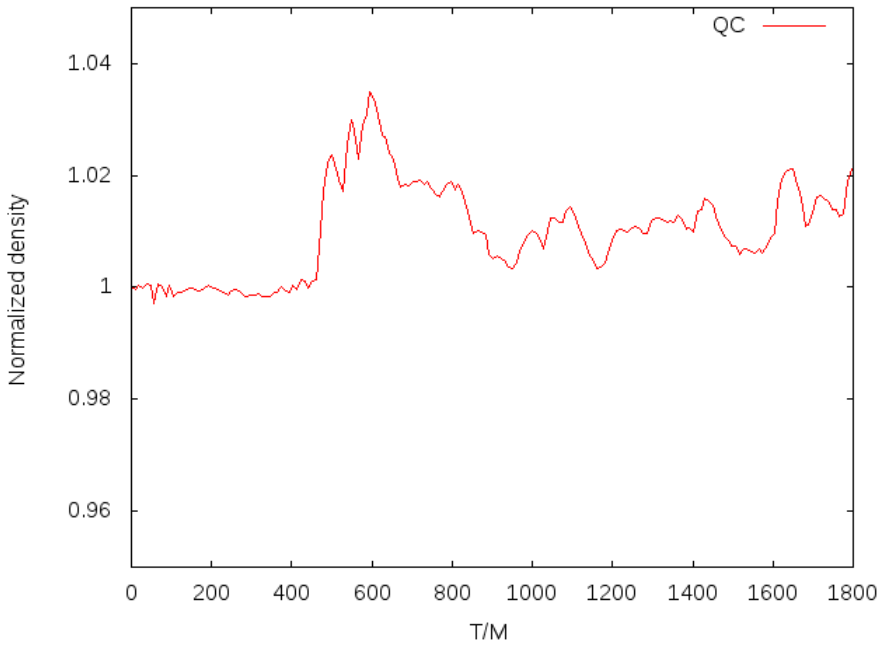

Figure 5.5: Central density oscillation of `LORENE` initial data. It show relatively large amplitude at coordinate time 600. When we run small central density, it delvers smaller amplitude around 1 percent. Therefore it is possible to think that higher central density may show large amplitude.

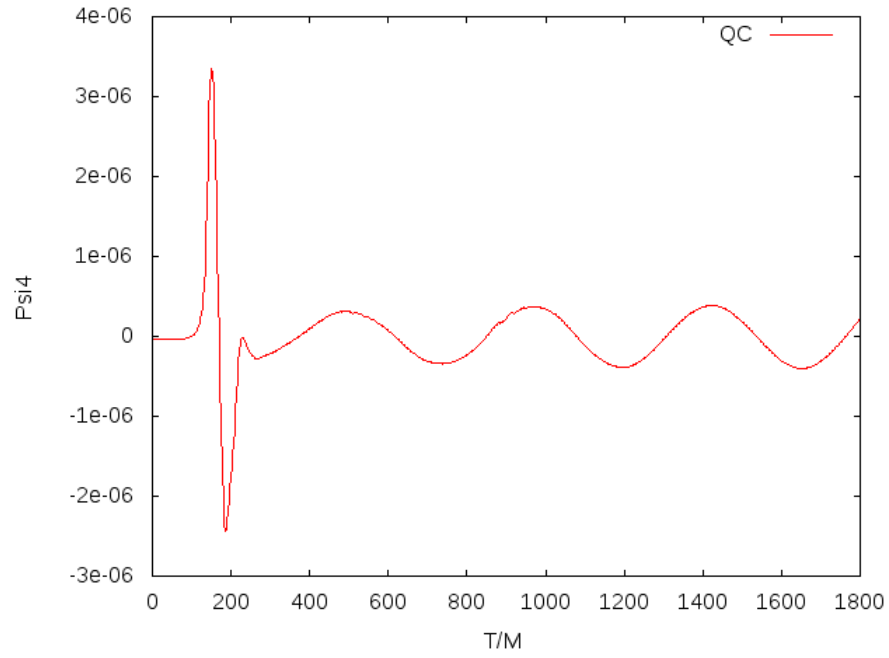

Figure 5.6: Gravitational wave(Ψ_4) from the `LORENE` initial data. First two peaks are junk radiation. This is sort of that system recognize the existence of binary. Such a junk can be removed by time integration.

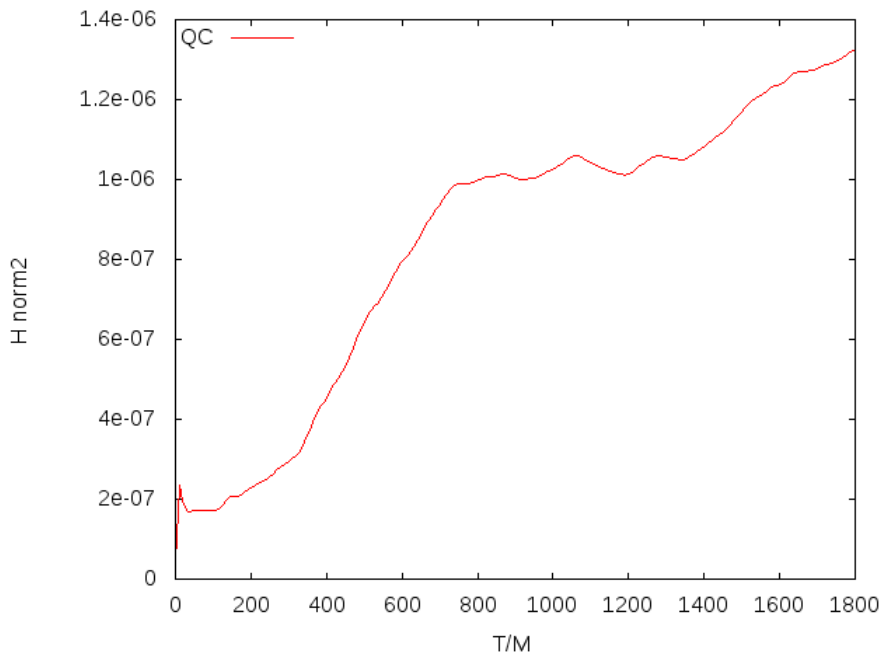

Figure 5.7: Constraint violation of hamiltonian. It gives how it deviates from 0. According to experience, about 10^{-6} to 10^{-7} is fairly enough accuracy.

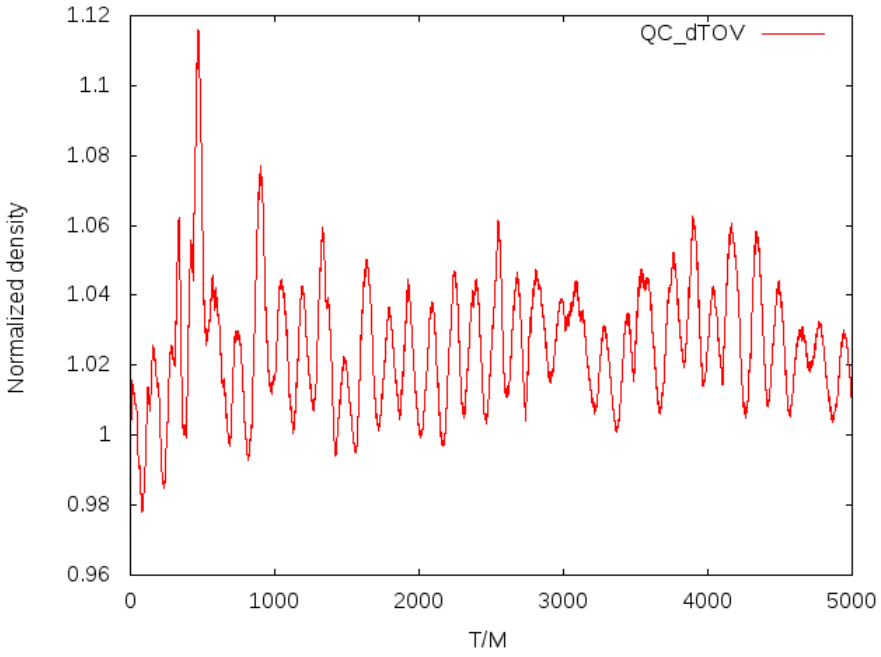

Figure 5.8: Normalized central density oscillation of binary TOV star. As you can see it has higher frequency mode and the amplitude is higher than results from `LORENE` initial data.

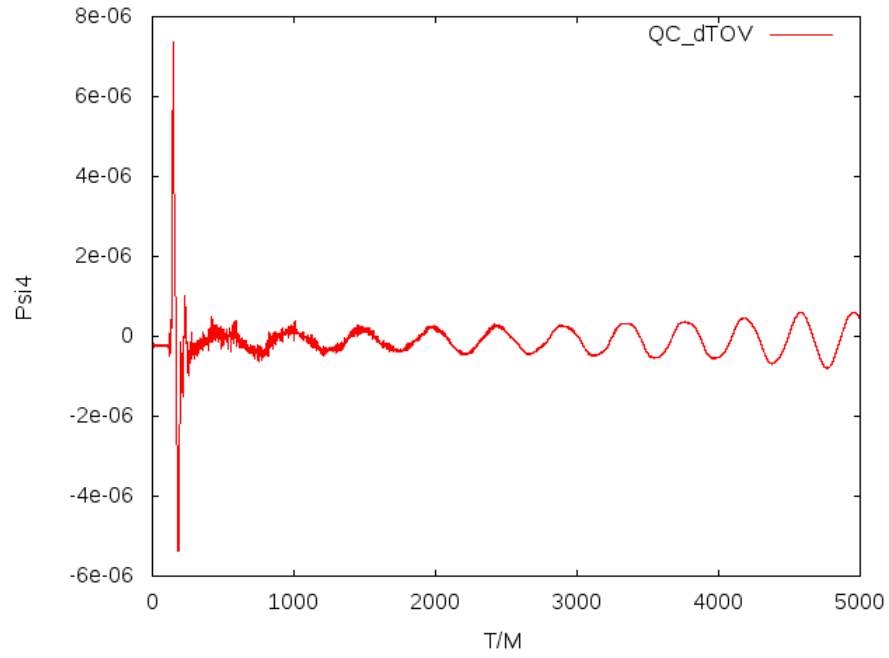

Figure 5.9: Gravitational wave from binary TOV star. It contains high frequency mode which might come from precession of TOV star itself. Such as phenomena is unphysical and the higher frequency mode tend to regulate starting at coordinate time 2000.

tend to increase as the binary system is evolving. But it still remains accurate level.

On the other hand, binary TOV star shows somewhat different physical aspect because it initially does not satisfy hydrodynamical equilibrium. TOV star is originally static and isolated solution but artificial boost and simple addition of companion spoils equilibrium state. Treatment to deal with such a situation will be introduced in next section in detail. Key difference between binary TOV and `LORENE` is high frequency mode in gravitational wave and central density oscillation. They seem to regulate as evolving.

5.4 Binary TOV stars

There are many ways to solve constraints equation which can provide useful initial data. But the system building initial data is too laborious and difficult so this section will show strategy in simple manner. Though this kind of method seem to be numerical trick, it might deliver physical insight thinking of perturbation.

5.4.1 Physical approximations

When TOV stars of head-on collision got booted in opposite direction respectively, they will not collide directly but make arbitrary orbit. An eccentricity of the orbit depends on magnitude of velocity or on its way of definition. One thing need to consider is rotating configuration because boosted object is not a point particle and fluid particle composed neutron star contains limited condition for viscosity. There is theoretical proof that viscosity of neutron star is not sufficiently large to build tidal locking. Besides dissipation time due to gravitational wave is shorter than time required to obtain tidal locking. Both of facts states that some rotation configuration which can trigger tidal locking is less likely to be physical. This kind of rotation configuration is corotating configuration, Figure 5.3.1 describe corotating neutron stars. Those are tidally locked so they always see same face of each companion like earth and moon. Also, deformation due to tidal interaction stay at fixed place until they got merged. When helical Killing

vector ξ^μ is given, fluid four velocity of corotating fluid particle is proportional to the Killing vector.

$$u^\mu_{\rm corot} = k\xi^\mu \tag{5.6}$$

Where k is constant factor. On the other hand, another extreme case of rotation config-

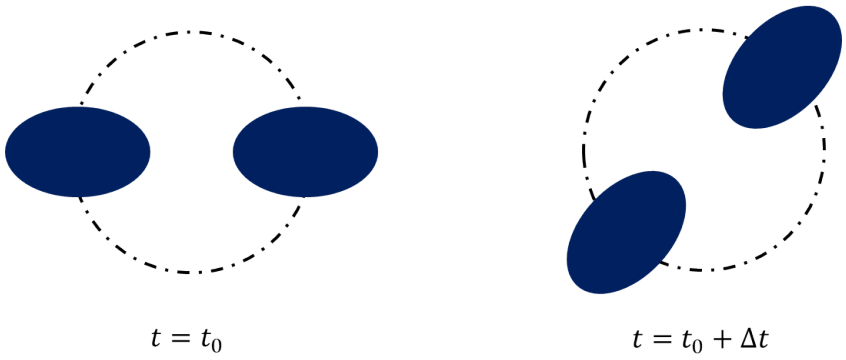

Figure 5.10: Corotating neutron star binary

uration is irrotational configuration. It is equivalent to vanishing vorticity as equation 2.2.45. No vorticity fluid particle keeps same shape of the neutron stars as initial one. Figure 5.3.2 expresses evolution of irrotational configuration and those figures show quite different phase of each configuration state. It is obvious that orbit evolution become different though initial data is exactly same. Irrotational configuration is relatively

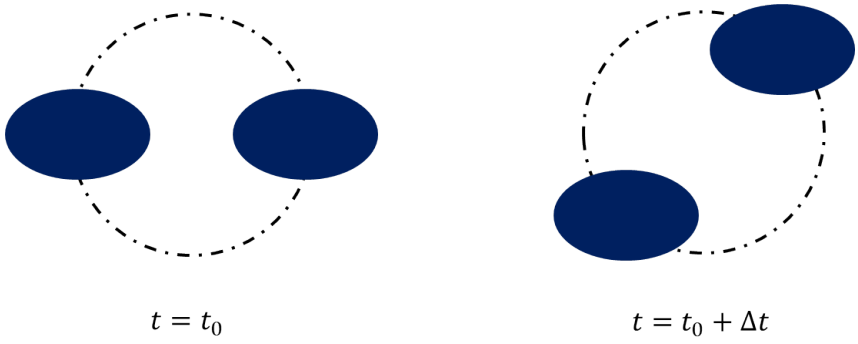

Figure 5.11: Irrotational neutron star binary

more physical than corotating one but it seems to be suspicious. When it rotates, tidal deformation should occur because of companion. Then one can say that the deformed

shape breaks down irrotational configuration. Of course, relativistic Kelvin-Helmholtz theorem asserts irrotational flow keeps vanishing circulation, i.e.,

$$u^{\mu}\nabla_{\mu}\mathcal{C} = 0 \tag{5.7}$$

where $\mathcal{C} = \oint hu_{\alpha}dx^{\alpha}$, relativistic circulation. The effect of deformation on vorticity may be another interesting topic to discover. With irrotational configuration, initial data contained such a fluid four velocity is necessary. By combining the equation 2.2.20, 2.2.47 and 2.2.48, stellar surface fitted four velocity can be obtained. Unfortunately, the equations are related to constraint equation therefore multi-grid method for solving elliptic equation is indispensable. There is alternative way to get approximately irrotatinal configuration. That is constant three velocity approximation(Moldenhauer et al. 2014), that is

$$\frac{u^i}{u^t} = const. \tag{5.8}$$

Literally, constant spatial coordinate velocity approximately behave as irrotational configuration at initial slice. Arranged approximation methods, maximum metric combination and constant three velocity, are likely to be crude way building up initial data. It seems to be but if those are fairly working, difficult and laborious way as solving elliptic equations employing multi-grid method can be detoured.

5.4.2 Low eccentricity

Not as much as superposed metric configuration, maximum metric configuration with boost show that spurious oscillation while two TOV stars are orbing each other. Though the system suppose helical symmetry, metric field do not know whether the symmetry is imposed or not. That is hydro variable story and that means it is not easy to make nearly quasi circular orbit. In general relativity, eccentricity is coordinate dependent quantity so there are many ways defining it. At this paper, eccentricity follows purely Newtonian definition.

$$\frac{r_f - r_c}{2a} \equiv e_i \tag{5.9}$$

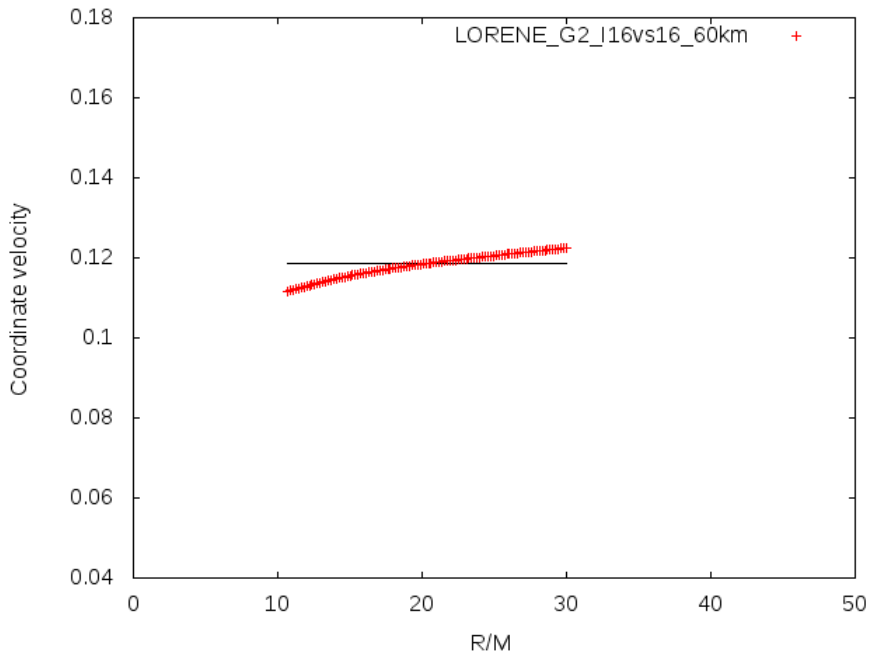

Figure 5.12: Example of constant three velocity approximation. LORENE is elliptic solver for constraint equations. Red dots represents irrotational fluid four velocity of $\Gamma = 2$ polytrope, 1.779 M_s at 60km coordinate separation in terms of coordinate velocity.

r_f is apoasteron, r_c is periasteron and a is major axis of the eccentric orbit. Due to gravitational wave of eccentric orbit, eccentricity is dissipated. e_i represents initial eccentricity comparing initial separation at apoasteron with periasteron appeared at the first time. Figure 5.3.4 shows the $e_i = 0.17$ orbit. Strange jump is appeared at the orbit in patches. Maybe density oscillation is attributed to the jump because it affects local density maximum. At the center, neutron star's trajectory is too concentrated. One thing to consider is the radius of the trajectory is smaller than radius of neutron star. Its true color is Hyper Massive Neutron Star(here after HMNS) which is hardly appeared in nearly head-on collision even if binary system is identical(everything is same except boost). According to Figure 5.3.5, large oscillation after coordinate time 3000 represents dynamical oscillation of HMNS. Nearly head-on collision has high eccentricity, it leads merge of the stars to direct black hole collapse. On the other hand, low eccentricity

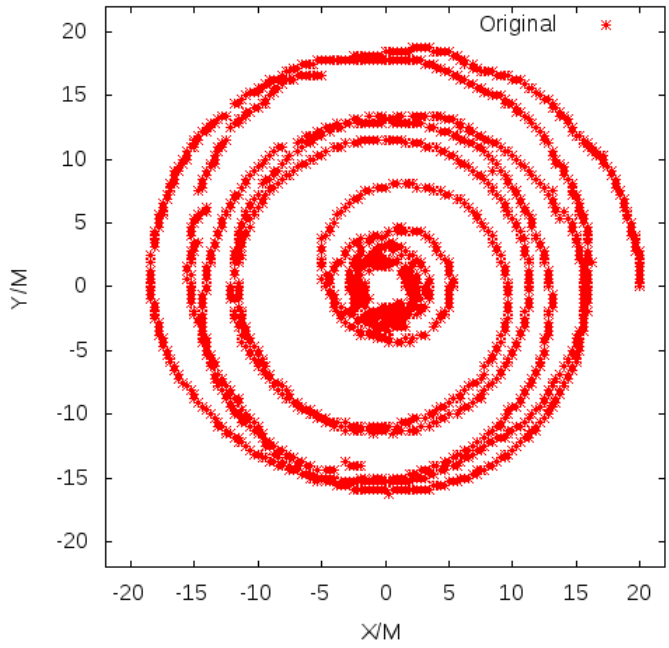

Figure 5.13: Orbit with low eccentricity. Many dots at the central region means violent rotation of HMNS.

requires characteristic velocity and ADM angular momentum to make bounded orbit. Such angular momentum trigger differential rotation configuration building up stability of HMNS which contains larger mass than typical mass of neutron star. An important thing to look at is inspiral phase of neutron star until 3000 coordinate time. There are two important problems one is spurious oscillation that contains strange amplitude and the other is constraint violation. Strange behaviour called spurious oscillation, as Figure 5.3.6 around 500 coordinate time, is unphysical so priority is removing this kind of error in valid way. Dominant cause triggering spurious oscillation is likely to be relativistic force balance because TOV star is originally static and stationary solution so external gravitational field or boost parameter spoils equilibrium state of isolated star solution. Employing maximum metric configuration, boost is only factor driving imbalance. In Newtonian interpretation, centrifugal force is added so equilibrium state need to be renewed. A strategy to find new profile of neutron star is injection energy

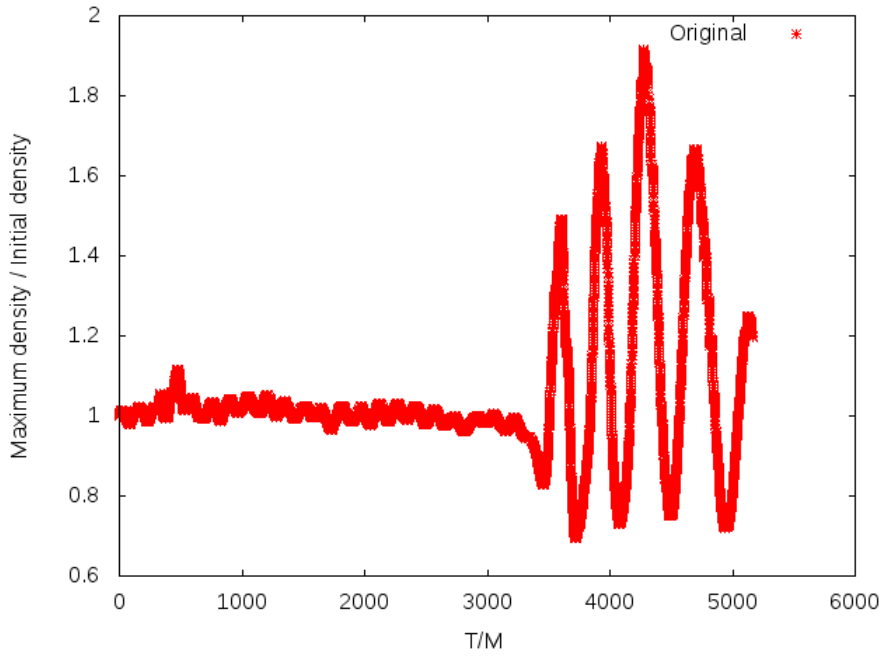

Figure 5.14: Maximum density oscillation of neutron stars until they merge. HMNS is appeared after coordinate time 3000.

which can be defined by helical Killing vector as Equation 2.2.43. When hydro variable shares same symmetry,

$$\mathcal{L}_\xi (hu_\mu) = \xi^\nu \Omega_{\nu\mu} + \nabla_\mu (hu_\nu \xi^\nu) \tag{5.10}$$

$$= 0 \tag{5.11}$$

Irrotation configuration ensure that vorticity tensor is vanished. Remained term,

$$\nabla_\mu (hu_\nu \xi^\nu) = 0$$

state homogeneous injection energy and it fulfils relativistic euler equation because

$$\nabla_\mu (hu_\nu \xi^\nu) = 0 \ \rightarrow \ u^\mu \nabla_\mu (hu_\nu \xi^\nu) = 0 \tag{5.12}$$

Another name of injection energy divergence free condition is strong Bernoulli's theorem. Therefore such a energy is conserved whole fluid world line. Binary TOV star of Figure 5.3.6 do not have homogeneous injection energy as "Original" in Figure 5.3.7. It

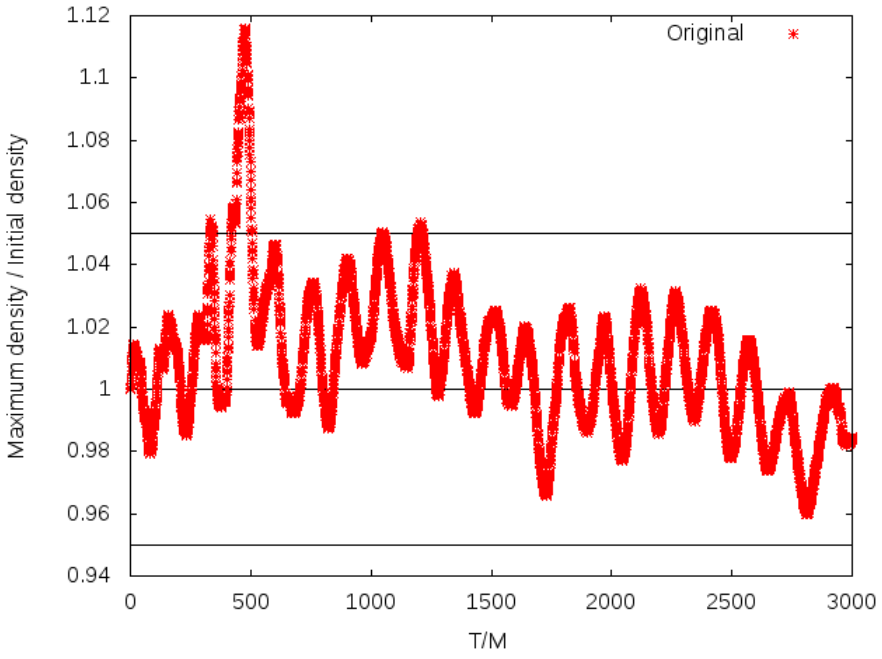

Figure 5.15: Maximum density oscillation of neutron stars while they are orbiting.

is necessary that enforcing homogeneity via perturbation, especially pressure perturbation. The perturbation insists pressure variation without density variation. It implies polytropic process breaks down instantaneously. Given helical symmetry, injection energy is defined as

$$E_{\text{inj}} = \alpha W \left(1 - \gamma_{yy} v^y v^y\right) h \tag{5.13}$$

Here, perturbed quantity is only enthalpy h.

$$-\left(h' - h\right) = \frac{\Gamma}{\Gamma - 1} K \left(\rho' - \rho\right) \tag{5.14}$$

Note that there is no deformation at initial slice so the boundary condition for perturbation is

$$\delta P \left(r = R\right) = \delta\rho \left(r = R\right) = 0 \tag{5.15}$$

A functional form of perturbation is following.

$$\delta\rho = -\frac{\Gamma - 1}{\Gamma K} \delta h \tag{5.16}$$

$$= \rho_0 f\left(r\right) \tag{5.17}$$

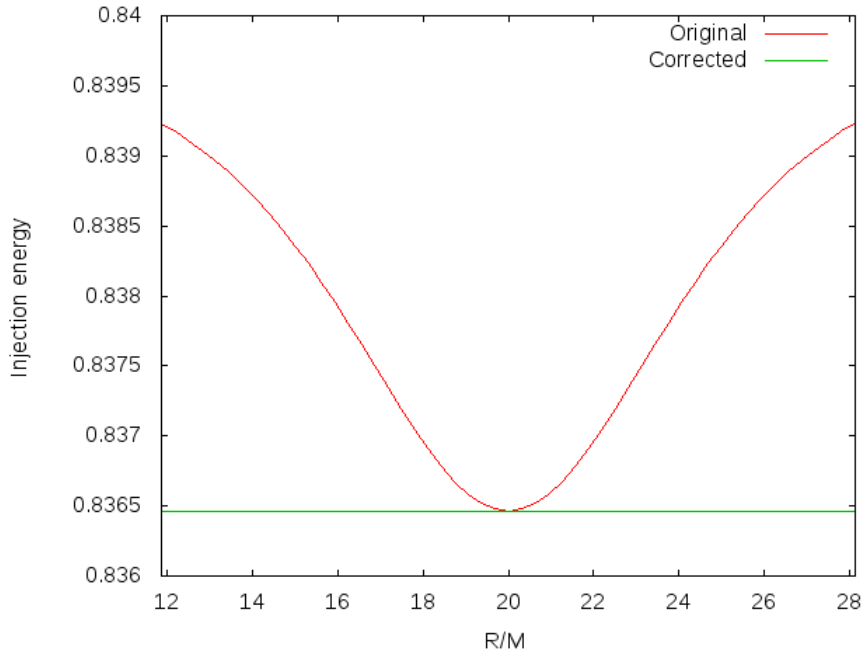

Figure 5.16: Example of injection energy. Red line implies neutron stars which contains spurious oscillation. Green line is recommended injection energy configuration. The difference between two injection energy delivers perturbation.

Due to boundary condition, applied perturbation is different as shown in Figure 5.3.8. This is one of limitations of perturbation method so homogeneity of injection energy is broken near surface. One more thing to think is choice of injection energy. The energy must be conserved but there is no specific value of it. From central injection energy to surface injection energy, many values are available. The degree of freedom problem need various evolution and the best evolution will be chosen. Injection energy is provided with respect to central enthalpy as following. According to injection energy configuration, pressure perturbation can be obtained to make such a quantity injected into stellar interior. When injection energy whose enthalpy is smaller than central one is applied, central density is reduced. This is reason why injection energy at boundary can not be chosen. It reduces central density too much so it can lead to another spurious oscillation.Each trial perturbation shows that similar evolution but different amplitude.

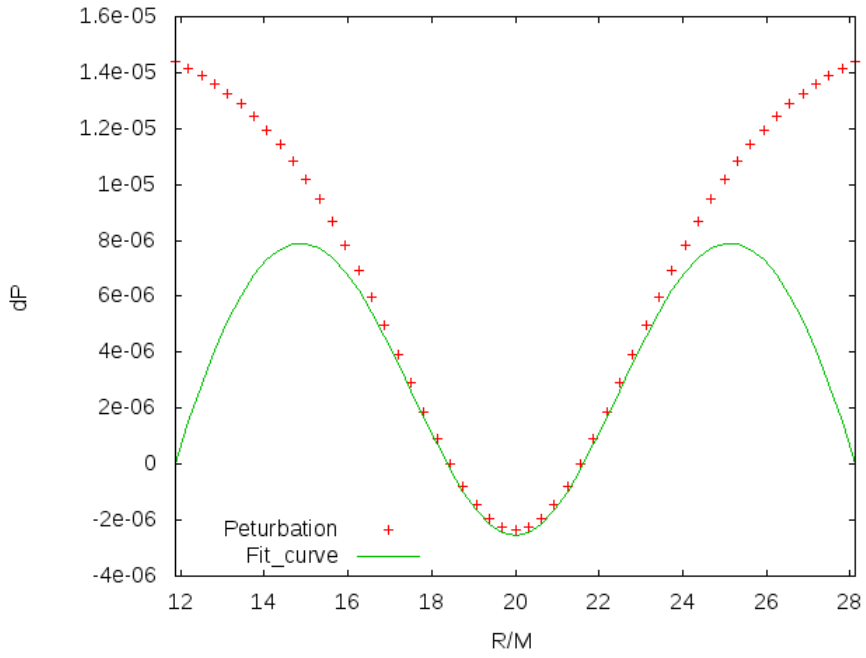

Figure 5.17: Example of perturbation applied. Due to boundary condition at the star surface, perturbed quantity on stellar radius should be zero.

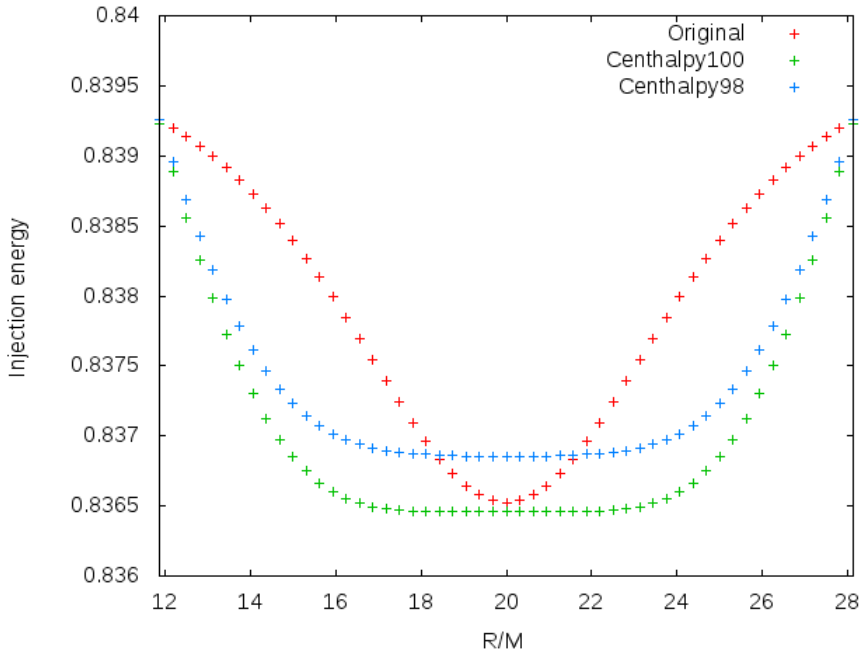

Figure 5.18: Trial injection energy. Centhalpy means central enthalpy and number 100, 98 represent percentage. The perturbation is applied with respect to central enthalpy.

Main objective is removing peak around 500 coordinate time. It seem to be ambiguous saying which evolution is better. But the important thing is relived peak around 500 coordinate time. Though perturbed one shows excited mode, its amplitude is at last 5 percent.

5.4.3 High eccentricity

Like head-on collision, orbit which contains high eccentricity shows nearly direct collision therefore its orbiting time is relatively short. Sudden increasing amplitude as Figure 5.3.6, it occurs at least coordinate time 500. It implies if the end time of orbit is smaller than 500 coordinate time, the system do not need perturbation. This fact may imply other cause like irrotation configuration while star is deforming can interrupt equilibrium state. Anyway, the orbits are shown as Figure 5.3.12. Arrows of the Figure 5.3.12 is trace of mass ejecta. Note that the trace emerges after binary neuron star col-

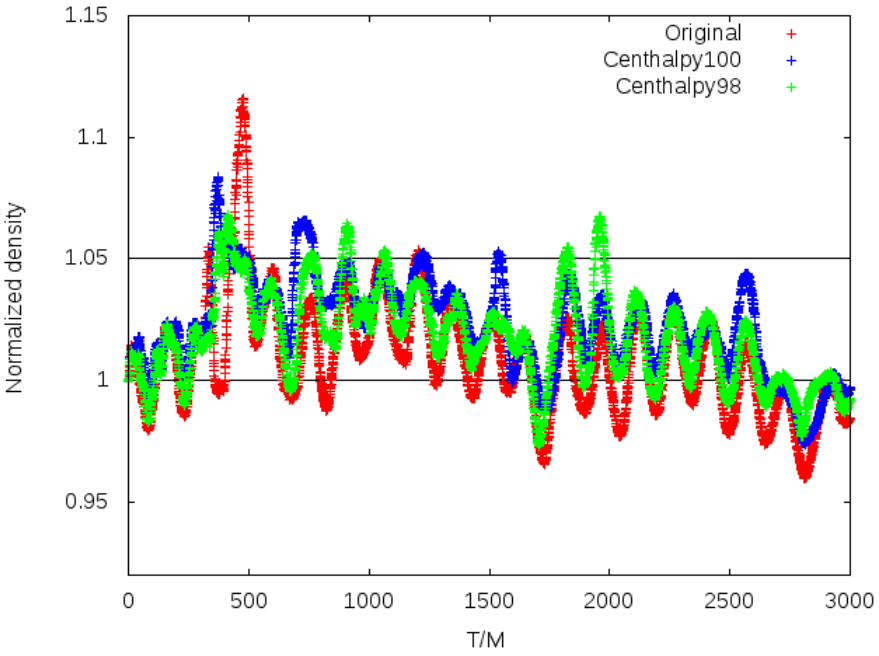

Figure 5.19: Normalized maximum density oscillation. Perturbation reduce spurious oscillation around the 500 coordinate time but it also make another mode.

lision, so density become very small comparing with the stars. Moreover it contribute gravitational interaction weakly with black hole. It composes disk near the black hole.

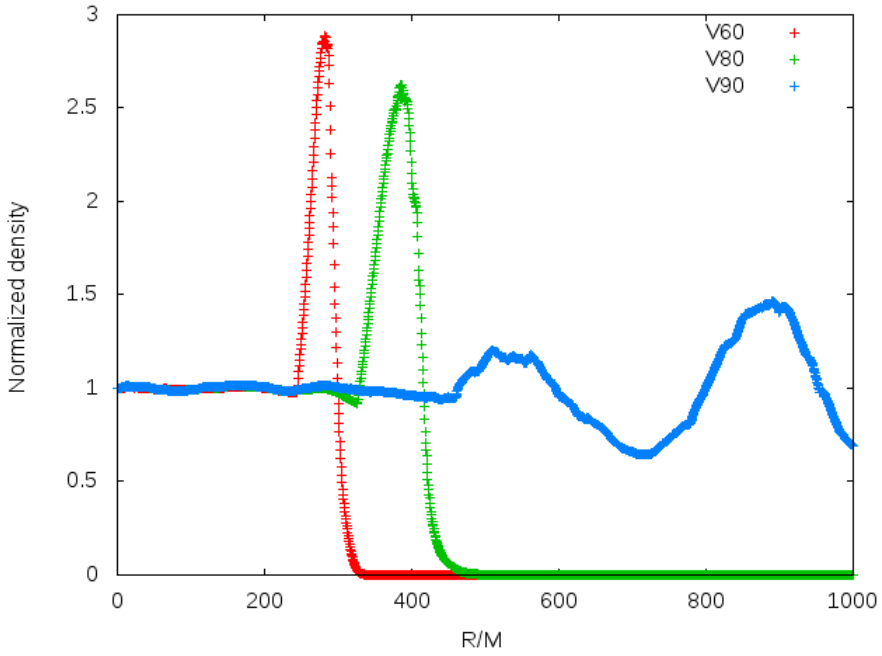

Figure 5.20: Maximum density oscillation normalized by initial maximum density. V is y direction velocity which make orbit lowly eccentric, 0.17, and number next to V means percentage of the velocity.

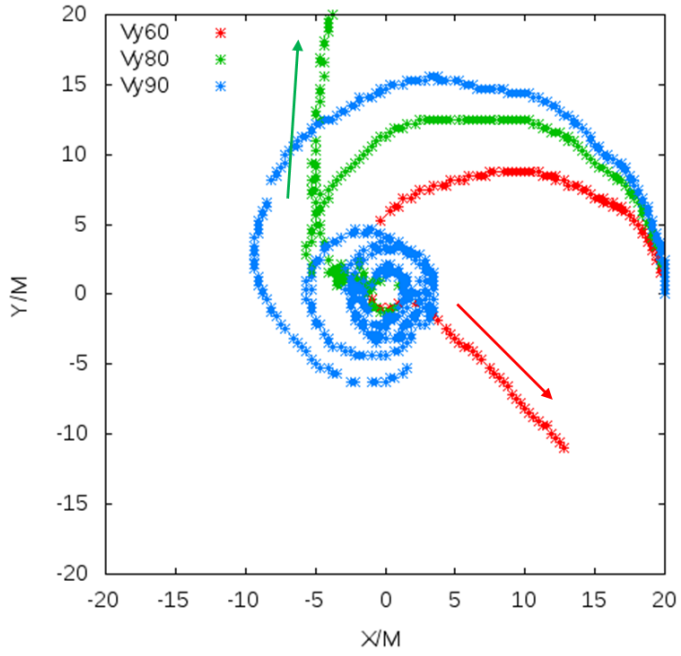

Figure 5.21: Highly eccentric orbit. In this situation, it is hard problem to define eccentricity.

Chapter 6

Conclusion

It is very difficult problem to solve initial data for general binary system though solution for quasi circular orbit is revealed. Here generality means general eccentricity of orbit. Employing double TOV star is suggested to build up such a general orbit but still has many issues. There are many reasons why eccentric orbit can not construct initial data as quasi circular orbit but main cause is that there is no current knowledge to define stationarity. For simplicity, this paper focuses on contribution of hydro variable such as pressure or density of the star rather than gravitation part to make fairly reliable initial data for eccentric orbit. It is not need to consider solving constraint equations for binary star or setting accurate initial metric field. First of all, TOV star which is the most important building block of binary system is static and stationary solution of Einstein's field equation. It assumes that following.

(i) TOV star is composed of perfect fluid.

(ii) Perfect fluid obeys polytropic process.

(iii) Metric field is spherical symmetric.

Those are key hypothesis of TOV star and is also one of origins of error for binary system. Spherical symmetry , i.e. static and stationary configuration can spoil physical characters of the binary. For instance, stars should be deformed because external gravity of companion star attracts fluid particle of main star. Moreover, TOV star solution

is originally static solution but binary system requires angular momentum so boost parameter also spoils it.

Therefore it is necessary that method to remove unphysical behaviour is required. Certain method is of course solving constraint equations for eccentric orbit but again, the objective is getting solution in simple way. Besides, there is no confidence solving constraints is able to provide 'good enough' solution. When double TOV stars are employed, main problem is first, spurious oscillation whose maximum density amplitude increases suddenly and second, relatively large constraint violation. To deal with the problems, new instruments is needed. Those are combination method of metric field and pressure perturbation via injection energy. Typically, superposed metric field is employed due to iterative algorithm and considering external field of companion at initial time slice. However, the method carrying out in the paper do not utilize iterative algorithm to get metric field. Maximum combination of metric field which ignore gravitation coming from partner is used so role of boost parameter is able to be revealed. For the boost, not every boost is available. TOV star ignores viscosity via perfect fluid assumption and it insists irrotational rotation configuration is physically true. Like constraint equations, irrotational configuration need elliptic solver and it is also detoured by using constant three velocity approximation. As binary system is evolving, it shows spurious oscillation and it can be reduced by pressure perturbation. Configuration of pressure perturbation is deduced from homogeneous injection energy. This conserved quantity asserts relativistic force balance so it suggest new pressure profile to make equilibrium.

$$\begin{aligned} g_{\mu\nu} &= g_{\mu\nu}|_1 + g_{\mu\nu}|_2 \\ \frac{u^i}{u^t} &= C \\ \nabla_\mu E_{\mathrm{inj}} &= 0 \end{aligned}$$

Bar next to metric represents maximum configuration.

As a result, pressure perturbation show fairly good behaviour by relieving spurious oscillation. It seems to be ambiguous but other evolution still shows amplitude at last 5

percent. Choice of injection energy effect on evolution because pressure variation should depend on the perturbation. Though Centhalpy100 relive spurious oscillation near 500 coordinate time less than Centhalpy98, it shows better oscillation at entire evolution. The LORENE case, elliptic solver for constraint equation in quasi circular orbit, show maximum density oscillation in the limit of 4 percent. But constraint violation is still large due to boundary line where each metric of TOV star meets. Metric point sharpening at the origin may be attributed to such a violation so it can be solved via lapse function smoothing.

Bibliography

bbott, B.P. et al. (LIGO Scientific Collaboration and Virgo Collaboration) 2016, Phys. Rev. Lett. 116, 061102

Abbott, B.P. et al. (LIGO Scientific Collaboration and Virgo Collaboration) 2017, Phys. Rev. Lett. 119, 161101

Alic, D., Kastaun W. and Rezzolla, L. 2013, Phys. Rev. D, 88, 064049

Andersson, N. and Comer, G.L. 2007, Living Reviews in Relativity, 10, 1

Baiotti, L., Hawke, I., Montero, P.J. Loffler, F., Rezzolla, L., Stergioulas, N., Font, J.A. and Seidel, E. 2005, Phys. Rev. D, 71, 024035

Baumgarte T.W. and Schmit B.G. 1993, Classical and Quantum Gravity, 10, 2067

Baumgarte T.W. and Shapiro S.L. 2010, Numerical Relativity, Cambridge

Brooker, R.A. and Olle, T.W. 1955, MNRAS, 115, 101B

Bona, C., Massó, J., Seidel, E. and Stela, J. 1995, Phys. Rev. Lett. 75, 600

Bonazzola, S. Gourgoulhon, E. and Marck J.-A. 1997, Phys. Rev. D, Vol 56, No. 12

Butterworth, E.M. 1976, ApJ, 204, 561B

Carter, B. and Gaffet, B. 1988, J. Fluid Mechanics, 186

Clark, M. and Laguna, P. 2016, Phys. Rev. D, 94, 064058

Chandrasekhar, S. 1964, ApJ, 139, 664C

Chandrasekhar, S. 1964, ApJ, 140, 417C

Friedman, J.L. and Stergioulas, N. 2013, Rotating Relativistic Stars, Cambridge

Giacomazzo, B. and Rezzolla, L. 2007, Classical and Quantum Gravity, 24, S235

Gourgoulhon, E., 2006, arXiv:gr-qc, 0603009v1

Gourgoulhon, E., Grandclement, P., Taniguchi, K., Mark, J.-A. and Bonazzola, S.

2001, Phys. Rev. D, 63, 064429

Gabler, M. Sperhake, U., and Andersson, N. Phys. Rev. D, 80, 064012

Gold, R., Bernuzzi, S., Thierfelder, M., Brügmann, B. and Pretorius, F.2012, Phys. Rev. D, 86, 12150

Hinderer, T. 2008, ApJ, 677, 1216-1220

Horedt, G.P. 2004, Polytropes, Astrophysics and Space Science Library

Lai, D, Rasio, F.A., Shapiro, S. L. 1993 ApJ, 88, 205L

Lai, D, Rasio, F.A., Shapiro, S. L. 1993 ApJ, 406L, 63L

Lichnerowicz, A. 1967, Relativistic Hydrodynamics and Magnetohydrodynamics, New York: Benjamin

Linblom, L. and Detweiler S.L. 1983, ApJ, 53, 73L

Loffler, F., Faber, J., Bentivegna, E., Bode, T., Diener, P., Haas, R., Hinderer, I., Mundim, B.C., Ott, C.D., Schnetter, Erik, Allen, G., Campanelli, M. and Laguna, P. 2012, Classical and Quantum Gravity, 29, 11

Misner, C.W., Thorne. K.S. and Wheeler, J.A. 1973, Gravitation, W.H. Freeman

Moldenhauer, N., Markakis, C.M., Jonhson-McDaniel N.K., Tichy, W. and Brugmann, B. 2014, Phys. Rev. D, 90, 084043

Owen, B.J. and Sathyaprakash, B.S. 1999, Phys. Rev. D, 60, 022002

Read, J.S., Lackey, B.D., Owen, B.J., and Friedman, J.L. 2009, Phys. Rev. D, 79, 124032

Rezzolla, L. and Zanotti, O. 2013, Relativistic Hydrodynamics, Oxford

Schnetter, E., Hawley, S.H. and Hawke, I. 2004, Classical and Quantum Gravity, 21, 6

Shibata, M., Taniguchi, K. and Uryu, K. 2003, Phys. Rev. D, 68, 084020

Smarr, L. and York, J.W. Jr. 1978, Phys. Rev. D 17, 2529

Taniguchi, K. 1999, Progress of Theoretical Physics, Vol. 101, No. 2

Tichy, W. 2009, Classical and Quantum Gravity, 26, 17

Thierfelder, M., Bernuzzi, S. and Brugmann, B. 2011, Phys. Rev. D, 84, 044012

Tooper, R.F. et al(IIT Research Institute) 1964, ApJ, 140, 434T

요 약

이 논문은 물질들로 채워져 있는 아인슈타인의 장 방정식을 새로운 방식으로 풀어내어 초기 조건을 구하고, 그 초기 조건을 진화시키는 데에 초점을 맞추고 있다. 적절한 초기 조건을 구하기 위해서 우리는 톨만 - 오펜하이머 - 볼코프 모델로 구성된 상대론적 별을 사용해 쌍성계를 구성하고 서로 반대방향으로 속도를 가해주었다. 이 모델로 구성되어 있는 상대론적 별은 완벽한 유체로 구성되어 있고, 폴리트롭이며 별이 구 대칭을 이루고 있다는 것을 전제로 삼고 있다. 따라서 정적이고 변화가 없는 상태이기 때문에 안정적인 밀도진동을 유지하고 있는 것이 물리적으로 정상적인 상태이다. 만일 이러한 상대론적 별이 어떤 힘에 의해서 가속이 되거나 속도를 갖게 된다면 안정적인 밀도진동을 깨지게 된다. 이렇게 생기는 밀도 진동은 정상상태를 보장하지 못하는 것이기 때문에 비물리적 오류이며 쌍성계를 이러한 정적인 별로 구성했을 때 발생할 수 있는 문제의 원인에 대한 힌트를 줄 수 있다.

우리는 정적인 상대론적 별을 활용해 타원 궤도를 돌고 있는 중성자별의 초기 조건을 만들었다. 별이 쌍성계를 구성하여 돌 때는 별을 구성하고 있는 유체 입자들이 어떠한 흐름을 타고 있는지 알아야하는데, 일반적으로 중성자 별 쌍성의 경우 와도가 0인 흐름인 비회전 흐름을 타게 된다. 비회전 흐름을 묘사하기 위해 좌표속도가 별 전체에 대해서 일정하다는 가정을 활용하였다. 또한, 쌍성이 구성되었을 경우 상대별에 대한 중력을 느끼에 될 텐데, 처음에는 중력을 느끼지 못한게끔 수치적으로 꾸몄다. 따라서 두 중성자 별의 메트릭 조합이 수치적 경계에서 마치 실로 기워져있는 형태라 생각하면 된다. 이렇게 얻는 초기 조건과 직접 아인슈타인 장방정식을 풀어서 얻은 초기 조건을 비교해 보았고, 중성자 쌍성이 초기에 평형 조건을 잘 맞추기 못해서 표면이 흔들려 생기는 높은 주파수의 진동이 생겼다.

쌍성계를 진화시키면서 이렇게 발생하는 이상한 진동은 이심률이 약 0.17 인 경우(작은 경우) 약 좌표시간이 500 근처에서 발생했다. 이심률이 큰 경우, 들뜨기 이전 시간에 충돌하게 되어 이상한 진동을 보이진 않는다. 움직이는 상대론적 별의 시뮬레이션 결과에 의하면 가해지는 속도가 이러한 높은 주파수 진동의 원인이라 파악했다. 상대론적 평형 상태가 속도에 의해서 깨지게 된 것인데, 다시 평형 상태래로 만들어 주기 위해 강한 베르누이의 법칙을 응용하여 압력에 대한 섭동을 줌으로써 별 내부에 균일한 삽입 에너지를

갖게 하는 방법을 취했다. 섭동이 가해진 쌍성계는 그 전보다 훨씬 경감된 밀도진동을 보여주었지만 완전히 바로잡는 역할을 해내지는 못했다. 또한 잠잠했던 부분이 오히려 들뜨게 하는(하지만 경계 값 이내의) 효과를 주기도 했다. 수치적 경계 부분에 바이올레이션 값이 올라가는 문제가 남아 있는데, 보외법을 통해서 해결 할 수 있으리라 본다.

주요어: 중성자 별: 초기 조건과 진화 – 중성자 별: 쌍성 – 중성자 별: 평형 상태 – 중성자 별: 수치 상대론

학 번: 2014-22382